Surface Science 675 (2018) 26–35

Contents lists available at ScienceDirect

Surface Science

journal homepage: www.elsevier.com/locate/susc

Molecular and dissociative adsorption of DMMP, Sarin and Soman on dry and wet TiO_2(110) using density functional theory

Yenny Cardona Quintero, Ramanathan Nagarajan*

Natick Soldier Research, Development & Engineering Center, 15 General Greene Avenue, Natick, MA 01760, United States

ARTICLE INFO

Keywords:
Adsorption of nerve agents on TiO_2
Molecular and dissociative adsorption
Dry and hydrated TiO_2
Slab model of TiO_2
DFT calculations of adsorption energy
Nerve agent dissociation mechanisms
Nerve agent and simulant comparison

ABSTRACT

Titania, among the metal oxides, has shown promising characteristics for the adsorption and decontamination of chemical warfare nerve agents, due to its high stability and rapid decomposition rates. In this study, the adsorption energy and geometry of the nerve agents Sarin and Soman, and their simulant dimethyl methyl phosphonate (DMMP) on TiO_2 rutile (110) surface were calculated using density functional theory. The molecular and dissociative adsorption of the agents and simulant on dry as well as wet metal oxide surfaces were considered. For the wet system, computations were done for the cases of both molecularly adsorbed water (hydrated conformation) and dissociatively adsorbed water (hydroxylated conformation). DFT calculations show that dissociative adsorption of the agents and simulant is preferred over molecular adsorption for both dry and wet TiO_2. The dissociative adsorption on hydrated TiO_2 shows higher stability among the different configurations considered. The dissociative structure of DMMP on hydrated TiO_2 (the most stable one) was identified as the dissociation of a methyl group and its adsorption on the TiO_2 surface. For the nerve agents Sarin and Soman on hydrated TiO_2 the dissociative structure was by the dissociation of the F atom from the molecule and its interaction with a Ti atom from the surface, which could indicate a reduction in the toxicity of the products. This study shows the relevance of water adsorption on the metal oxide surface for the stability and dissociation of the simulant DMMP and the nerve agents Sarin and Soman on TiO_2.

1. Introduction

Chemical warfare agents (CWA) are highly toxic molecules that represent a lethal risk for the military and civilian personnel in zones of armed conflict and war as well as in the event of acts of terrorism [1–4]. Among the most lethal CWA are the organophosphate (OP) nerve agents whose lethality comes from the compound's ability to bind to the enzyme acetylcholinesterase (AChE) in the nervous system [1]. The nerve agents phosphorylate the active site of serine residue in the enzyme, rendering it inactive, thereby preventing the enzymatic breakdown of the neurotransmitter acetylcholine. The accumulation of acetylcholine causes continuous nerve impulses and muscle contractions and the victim can suffer from convulsions, brain seizures, respiratory failure and eventually death. Two decades after the Chemical Weapons Convention that comprehensively prohibited the development, production, stockpiling, transfer and use of chemical weapons, the nerve agents continue to be used in war zones as seen in the ongoing Syrian conflict, causing civilian and military fatalities [5]. Many countries also have stockpiles of nerve agents which have not yet been destroyed, posing potential threat of their use. In order to protect the Soldier and the civilian population, to decontaminate battlefield equipment and infrastructure and to ensure remediation of environments exposed to these chemical agents, the exploration and development of materials with propensity to efficiently adsorb and degrade nerve agents is imperative.

Experimental studies in the literature on surface adsorption and decomposition using nerve agents are limited due to their high toxicity. Instead, molecules with similar chemical and physical properties to the CWA but with less toxicity, selected as simulants, have been used as substitutes to understand the properties of the nerve agents when adsorbed on surfaces [2]. Theoretical methods, such as density functional theory (DFT) represent an important tool to investigate the atomic properties of the nerve agents as well as simulants and their interaction with surfaces, allowing a better understanding of the atomic and surface properties of the agent-surface system and also the validity of agent-simulant correlations.

Various detection and decontamination methods for nerve agents have been explored, with metal oxides surfaces showing promising results due to their selectivity in the sensing and decontamination process and the large number of active sites being available [1–4].

* Corresponding author.
E-mail address: ramanathan.nagarajan.civ@mail.mil (R. Nagarajan).

https://doi.org/10.1016/j.susc.2018.04.002
Received 3 January 2018; Received in revised form 30 March 2018; Accepted 8 April 2018
Available online 21 April 2018
0039-6028/ Published by Elsevier B.V.

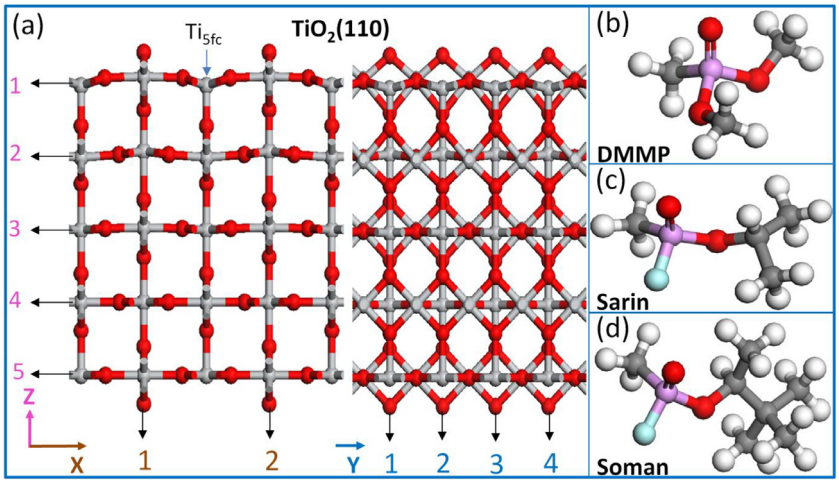

Fig. 1. Surface and molecules modeled in this work (a) TiO_2(110) rutile in the *xz* (left) and *yz* (right) views with 80 TiO_2 groups and 5 layers, (b) simulant DMMP, (c) nerve agent Sarin, and (d) nerve agent Soman.

Metal oxide surfaces including MgO, CaO, Al_2O_3, La_2O_3, Fe_2O_3, MoO_3, CuO, $Zr_4(OH)_{16}$, CeO_2, SiO_2, SnO_2, ZnO and TiO_2 have been explored for the adsorption of nerve agents and simulants on surfaces using both experimental and theoretical methods [1–4,6–40]. Among the theoretical methods, DFT has been widely used to obtain valuable information on the interaction between the nerve agent and the metal oxide surfaces as well as on the stability and structure of the agent [6–13]. In spite of the numerous metal oxide materials explored, their instability represents an important limitation for practical applications. TiO_2 among the metal oxides, has shown promising characteristics for the adsorption and decontamination of nerve agents, due to its high stability and rapid decomposition rates [1]. Previous studies on the adsorption of Sarin on TiO_2 found the catalytic decomposition of the nerve agent on the hydrated TiO_2 to be a plausible method for the decontamination of Sarin [1,2,20,41]. However, a systematic theoretical and comparative study of the adsorption and decomposition process of nerve agents and simulants on a model metal oxide, such as TiO_2, as well as their stability and dissociative structure has not been reported, to the best of our knowledge. In addition, the effect of environmental conditions, especially the hydration of the surface, on the stability and dissociative structures of the nerve agents remains unclear. The examination of these factors will significantly contribute to our understanding of the nerve agents' decontamination process. Also a study of the similarities between nerve agents and their simulants will help verify agent-simulant correlations and determine the validity of extrapolation of experimental results on simulants to the actual nerve agents.

In this work, we have studied the adsorption of the nerve agents Sarin (isopropyl methylphosphonofluoridate) and Soman (pinacolyl methylphosphonofluoridate) and the simulant DMMP (dimethyl methylphosphonate) on a dry and wet TiO_2(110) slab surface using DFT. We calculated the adsorption energy and geometry of the molecular and dissociated agents on TiO_2(110). The effect of H_2O adsorption on the surface was also considered by the comparison of dry and wet TiO_2 surface properties. For the wet system, computations were done for the cases of both molecularly adsorbed water (hydrated conformation) and dissociatively adsorbed water (hydroxylated conformation). We found that the dissociative adsorption of the agents is preferred over the molecular one for both dry and wet systems. The dissociative structure for DMMP on TiO_2(110) showed a significant variation from those for the nerve agents Sarin and Soman. In the case of the wet systems, the hydration and hydroxylation of the TiO_2(110) surface were considered with the dissociative adsorption of the agents on the hydrated TiO_2 surface being more stable than for the hydroxylated one. Lastly, the final structures of the agents on TiO_2(110) were also obtained and described for the different systems considered here.

2. Computational methods

The DFT calculations were carried out with the Quantum Espresso software [42], with the Perdew–Burke–Ernzerhof (PBE) generalized gradient approximation (GGA) [43] and the projected-augmented wave (PAW) [44] approach. Van der Waals interactions were taken into account using the DFT-D2 method of Grimme [45]. GGA-PBE has shown to have good accuracy in the description of adsorption energetic and water bonds [46]. In addition, accounting for van der Waals forces has shown to increase the adsorption strength of molecules with the surface. The cutoff kinetic energy for the wave functions and the charge density were 30 Ry (1 Ry ≈ 1312.75 kJ/mol) and 350 Ry, respectively. These parameters were selected following the pseudopotential suggestions for the different atom types found in each system studied.

2.1. TiO_2 parameters

The TiO_2 bulk lattice parameters were calculated using a k-mesh of 8 × 8 × 10 k-points. The final a and c lattice parameter values were calculated to be 4.6408 Å and 2.9683 Å, respectively, showing good agreement with previous theoretical and experimental studies [7,47]. The TiO_2(110) rutile slab structure (the most thermodynamically stable phase of TiO_2) was constructed with a surface area of (2 × 4) corresponding to 13.126 Å × 11.873 Å. Five TiO_2 layers and a total of 80 TiO_2 groups or 240 atoms and a vacuum region of 12 Å was adopted (Fig. 1(a)). The two bottom layers were fixed at their bulk position and the three top layers were allowed to relax.

2.2. Initial configuration of molecules on TiO_2 surface

The initial structures for the agents, DMMP ($C_3H_9O_3P$), Sarin ($C_4H_{10}FO_2P$) and Soman ($C_7H_{16}FO_2P$) were built based on the geometries reported in the literature [48–50]. Different conformers for DMMP, Sarin and Soman were considered to determine the most stable configuration. The different molecules were relaxed using the free molecule method until reaching the most stable geometry. The final structures for DMMP, Sarin and Soman are observed in Fig. 1(b), (c) and (d), respectively. The agent-TiO_2 systems were built with 1 molecule per 8 Ti atoms 5 fold coordinated (Ti_{5fc}), with a surface area of (2 × 4), five TiO_2 layers (Fig. 1a), and a total of 80 TiO_2 groups. The agents were placed on top of TiO_2(110) creating an asymmetric slab which requires the dipole correction to account for the artificial field in the system due to the periodicity of the lattice. A vacuum region between 8 and 25 Å was tested for the adsorption of the agents on the TiO_2(110) slab described previously. For vacuum sizes between 12 and

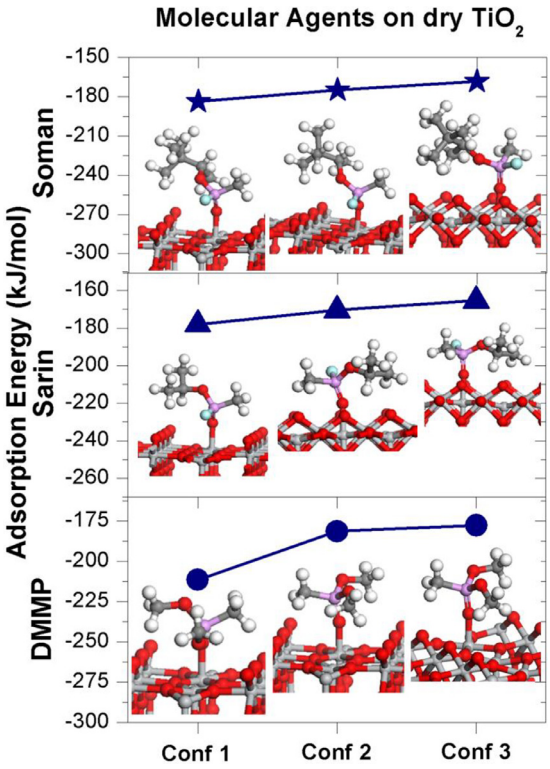

Fig. 2. Adsorption energy in kJ/mol and structure of DMMP (circle), Sarin (triangle) and Soman (star) on the TiO_2(110)surface. The results shown are for the three lowest energy conformations.

25 Å, the atoms positions and adsorption energy remained stable. A minimum vacuum region of 12 Å was selected after testing its ability to avoid interactions of the molecule with adjacent periodic images. Different possible adsorption configurations of the molecule on the dry TiO_2(110) slab were included (shown in Supporting Information S1–S6). The selection of the configuration was based on the possible arrangements of the molecule on the TiO_2(110) surface including distance to the surface, bond lengths, bond angles, possible secondary bonds formed and orientation of the molecule respect to the surface. Additional initial configurations of the agents on the TiO_2(110) surface were also constructed based on the geometry reported in previous works as stable systems [7,8].

2.3. TiO_2 under wet conditions

Agent-TiO_2 systems under wet conditions were built to determine the effect of H_2O on the adsorption of agents on the TiO_2(110) surface. The adsorption of H_2O on TiO_2(110) was considered with both a hydrated and hydroxylated configuration with a coverage of 0.5 H_2O monolayer. In the hydrated surface, the H_2O molecules were adsorbed on the top TiO_2 layer forming a bond with the Ti_{5fc} surface atoms. In the hydroxylated configuration, H_2O was dissociated into OH and H, the OH groups were adsorbed on the Ti surface atoms while the H atoms adsorbed on the adjacent O surface atoms. The information from previous experimental and theoretical studies was used to construct and model the TiO_2–H_2O interface [51–53]. The adsorption of DMMP, Sarin and Soman on the wet TiO_2(110) surface was modeled using the same slab systems described for the dry configurations. The initial agent-TiO_2 structures of the wet systems are shown in Supporting Information (S7–S18).

3. Results from DFT calculations

3.1. Adsorption of DMMP, Sarin and Soman on dry TiO_2(110)

DMMP, Sarin and Soman (Fig. 1(b), (c) and (d), respectively) can adopt different configurations after adsorption on the TiO_2(110) surface. The adsorption of the agents on TiO_2 has been reported in different studies for both molecular and dissociative conformations. In the former, experimental and theoretical works have described the interaction of the P═O group in DMMP and Sarin with the Ti_{5fc} atoms on the TiO_2(110) surface as the preferred adsorption configuration of the molecular agents on this surface [7,41]. In the latter, conversely, different dissociative products can be expected, especially due to the variation in composition and the environmental factors that influence the dissociative process. Different initial adsorption configurations of the agents, DMMP, Sarin and Soman on the dry TiO_2(110), with molecular and dissociative configurations were explored in the initial part of this work and are shown in Supporting Information (S1-S6). After the energy minimization was finalized and the convergence criteria were achieved, the most stable configurations were determined.

3.1.1. Molecular adsorption of DMMP, Sarin and Soman on dry TiO_2(110)

Among the initial configuration explored in the molecular adsorption of the agents on TiO_2 are the formation of monodentate and bidentate configurations with the O atoms from the agents forming bonds with the TiO_2 surface. Also, different possible interactions of the F atom from Sarin and Soman with the TiO_2 surface were considered (shown in Supporting Information S1–S3). The adsorption energy (E_{ads}) was determined for each one of these agent-TiO_2 modeled systems for DMMP, Sarin and Soman. The E_{ads} calculation for the each configuration of the agent-TiO_2 system can define its relative stability and the most preferred structure. The E_{ads} for the molecular adsorption of DMMP, Sarin and Soman on TiO_2(110) can be defined as:

$$E_{ads} = E_{Agent-TiO_2(110)} - E_{TiO_2(110)} - E_{Agent} \quad (1)$$

where $E_{Agent-TiO_2(110)}$ corresponds to the energy of the agent adsorbed on the TiO_2(110) surface, $E_{TiO_2(110)}$ is the energy of the clean TiO_2(110) surface and E_{Agent} is the energy of the gas phase isolated agent (DMMP, Sarin or Soman). The E_{ads} for the molecular adsorption of the agents on TiO_2 was calculated for the different adsorption configurations shown in Supporting Information (S1–S3). The three lowest E_{ads} values for the molecular adsorption of DMMP, Sarin and Soman on TiO_2(110) and their final structures are shown in Fig. 2. The lowest E_{ads} of the agent-TiO_2 were −221.4, −178.0 and −183.7 kJ/mol for DMMP, Sarin and Soman, respectively. The difference in the lowest E_{ads} between the simulant DMMP and the CWAs (Sarin and Soman) was ~30 kJ/mol, while the same property showed a difference between Sarin and Soman of only 6 kJ/mol. In the preferred molecular configuration, a covalent bond is formed between the P═O group of DMMP, Sarin and Soman and the Ti_{5fc} atom of the TiO_2 surface as reported also in previous works for DMMP on TiO_2, as well as Sarin and VX on other metal oxide surfaces [6-8,11]. The monodenate Ti−O configuration was preferred over the bidentate ones (two Ti−O bonds or a Ti−O and a Ti−F bond), also considered as initial conformations.

Previous theoretical works in the literature have also reported the E_{ads} of the nerve agents Sarin and the simulant DMMP on metal oxides. For DMMP and Sarin on TiO_2, they reported E_{ads} values of −125.4 kJ/mol for both molecules. However, these studies considered the adsorption of the agents on a TiO_2 cluster. It has been shown that the cluster models of TiO_2 over or under-estimate the E_{ads} compared to the slab systems, especially for small cluster sizes [6,34]. Other important difference between the methods used in this work and previous reported works is the application of the DFT-D functional to calculate the E_{ads}. The DFT-D method accounts for van der Waals interactions in the system after adsorption of the agent on TiO_2. In our calculations, there was a difference of around 50 kJ/mol for the systems including van der

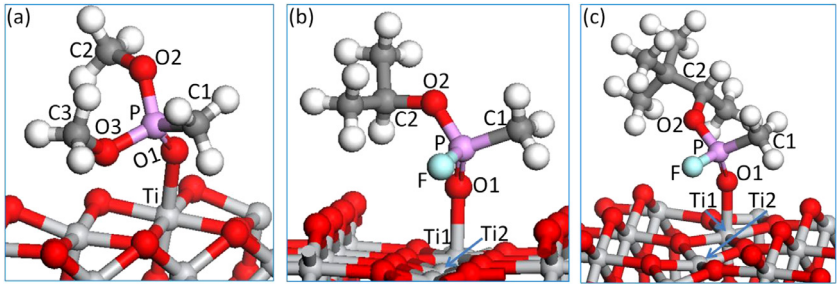

Fig. 3. Stable geometry and orientation of molecularly adsorbed agents on TiO_2 for (a) DMMP, (b) Sarin, and (c) Soman.

Table 1
Values for the geometric parameters of molecularly adsorbed agents DMMP, Sarin and Soman on TiO_2. Refer to Fig. 3 to find the atomic description.

Geometric parameter	DMMP-TiO_2 refer to Fig. 3a	Sarin-TiO_2 refer to Fig. 3b	Soman-TiO_2 refer to Fig. 3c
Bond length (Å)			
O1−Ti1	2.09	2.12	2.08
O1−P	1.50	1.50	1.49
O2−P	1.57	1.56	1.56
O3−P	1.61		
C1−P	1.78	1.78	1.78
C2−O2	1.46	1.50	1.49
C3−O3	1.46		
P−F		1.59	1.57
Ti2···F		3.16	3.60
Bond angle (°)			
Ti1−O1=P	139	142	152
O1−P−F		108	111
H bonds			
No. of H bonds	5	3	3
H(CH_3)−O(TiO_2)	2.22–2.99	2.52–2.56	2.53–2.62

Waals corrections compared to the one that did not account for these interactions.

Fig. 3 and Table 1 show the geometric parameters calculated for the agent-TiO_2 systems for the molecular adsorption of DMMP, Sarin and Soman on TiO_2 with the most stable configuration. In general, the bond lengths and bond angles for the different agents-TiO_2 systems had similar values. The only parameter that showed a considerable distinction between the simulant and the nerve agents was the number of H bonds (secondary bonds formed between an H atom of the molecule and an O at the TiO_2 surface). The DMMP-TiO_2 system has 5 H bonds, while the systems with the nerve agents Sarin and Soman have 3, as observed in Table 1.

The comparison of the number of H bonds between the systems with various E_{ads} suggests that the number of H bonds has an important influence over the stability of the agent-TiO_2 systems in a molecular configuration. For the most stable DMMP, Sarin and Soman adsorbed on TiO_2, the configuration with higher number of secondary bonds corresponds to the most stable one. In the most stable agent-TiO_2 systems there are 5, 3 and 3 H bonds for DMMP, Sarin and Soman, respectively, while for the less stable configurations there are only between 1 and 2 H bonds.

Another important interaction in the most stable structures of nerve agents Sarin and Soman is the position of the F atom, above a Ti_{5fc} surface atoms (close to an "atop" position). The Ti···F distance in the nerve agents suggests that there is not an actual bond formed between F and Ti_{5fc} but instead, a weak interaction could take place between both atoms, which could have an effect on the stability of the structure.

3.1.2. Dissociative adsorption of DMMP, Sarin and Soman on dry TiO_2(110)

One of the relevant factors in the decontamination process of CWA is the possible dissociation of the agents when adsorbed on metal oxide surfaces. During the adsorption process, different dissociation products can be formed, reducing in some cases the toxicity of the nerve agents. In this work, different possible dissociation products were considered (shown in Supporting Information S4–S6). Among the initial configurations, the dissociation of one or two methyl groups from DMMP was considered. For Sarin and Soman the formation of CH_3PO_2F with the dissociation of the remaining group, or the dissociation of the F atom from the nerve agent were some of the initial dissociative structures modeled. Among the different configurations, the three lowest E_{ads} for the most stable dissociated DMMP, Sarin and Soman on TiO_2(110) are shown in Fig. 4, along with the final geometric configurations for the different systems. The E_{ads} definition in Eq. (1), can be extended to the dissociative adsorption of the agents on TiO_2, with the $E_{Agent-TiO_2(110)}$ term corresponding to the energy of the dissociative agents on TiO_2(110). The lowest E_{ads} for DMMP, Sarin and Soman on TiO_2 in a dissociative configuration were −281.3, −260.3 and −285.4, respectively. Even though the E_{ads} difference of the dissociative adsorption for the simulant compared to the nerve agents is only 20 kJ/mol, the structure for the final dissociated products has a significant difference

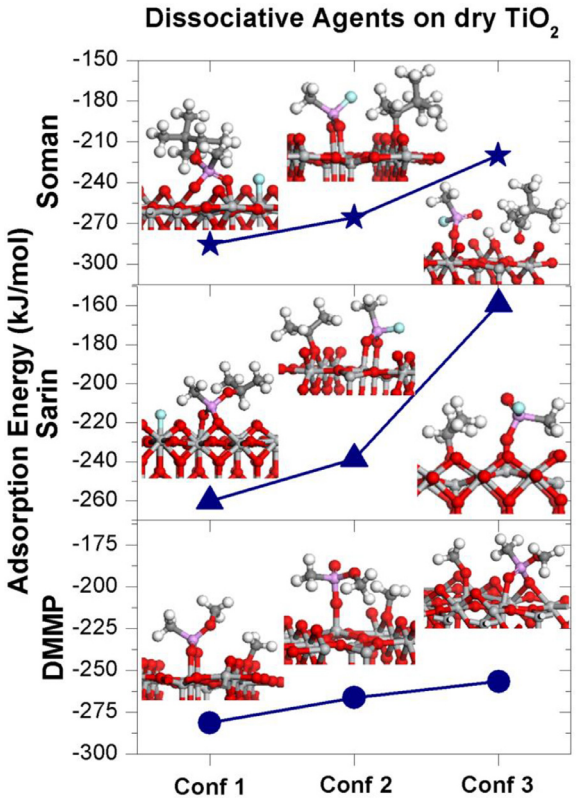

Fig. 4. Adsorption energy in kJ/mol and structure for the dissociative adsorption of the agents of DMMP (circle), Sarin (triangle) and Soman (star) on the TiO_2(110) surface. The results shown are for the three lowest energy conformations.

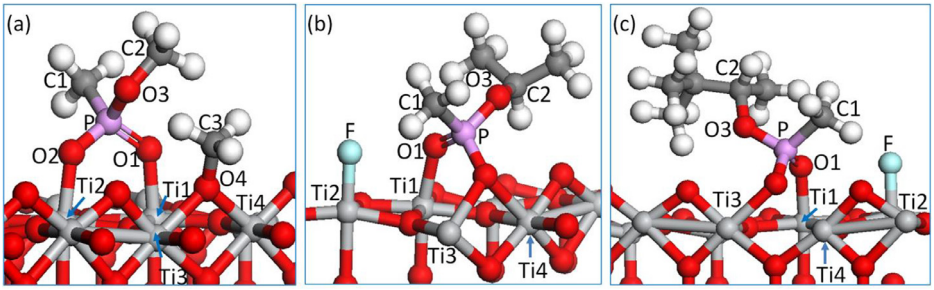

Fig. 5. Stable geometry and orientation of dissociatively adsorbed agents on TiO_2 for (a) DMMP, (b) Sarin and (c) Soman.

Table 2
Values for the geometric parameters of dissociatively adsorbed agents DMMP, Sarin and Soman on TiO_2. Refer to Fig. 5 to find the atomic description.

Geometric parameter	DMMP-TiO_2 refer to Fig. 5a	Sarin-TiO_2 refer to Fig. 5b	Soman-TiO_2 refer to Fig. 5c
Bond length (Å)			
O1−Ti1	2.00	2.00	1.98
O2−Ti2	2.00		
O2−Ti3		2.20	2.20
O2−Ti4		2.30	2.30
O1−P	1.54	1.55	1.54
O2−P	1.54	1.57	1.56
O3−P	1.60	1.58	1.58
C1−P	1.79	1.79	1.79
C2−O3	1.44	1.48	1.48
Dissociated molecule bond length (nm)			
C3−O4	1.42		
O4−Ti3	2.09		
O4−Ti4	2.00		
F−Ti2		1.79	1.79
Bond angles (°)			
Ti1−O1═P	130	126	127
Ti2−O2═P	128		
Ti3−O2═P		124	123

for DMMP compared to Sarin and Soman.

For DMMP, a $(CH_3)_2O_3P$ main molecule in a bidentate configuration (two O atoms, each one binding with a Ti_{5fc} surface atom) and a CH_3 dissociated group is obtained as the dissociative structure. In the case of the nerve agents, the dissociative adsorption generates different products, with Sarin and Soman dissociated in a $(CH_3)_xC_yHO_2P$ group ($x = 3$, $y = 1$ for Sarin and $x = 5$, $y = 2$ for Soman) adopting a bidentate configuration and the F atom adsorbed on a Ti_{5fc} surface atom, leaving a less-toxic phosphonate product, as observed in Fig. 4. The $(CH_3)_xC_yHO_2P$ group from Sarin and Soman binds with an O surface atom of TiO_2 in order to form a bidentate configuration that leads to a stoichiometric conformation. The monodentate configuration of the main molecule was also considered as a sub-product of the dissociation for the different agents but in this case, less stable systems (higher E_{ads}) compared to the bidentate configuration were observed. The formation of CH_3PO_2F with the dissociation of the remaining group from Sarin and Soman was explored as well, resulting in a higher energy than the dissociation of the F atom. Additional different initial dissociative configurations of the agents on TiO_2 were studied as shown in the Supporting Information (S4–S6), some of them being unstable after relaxation of the system.

A comparison of the molecular and dissociative adsorption of DMMP, Sarin and Soman on TiO_2, showed that in general, the dissociative adsorption of the agents on TiO_2 is more stable than the molecular adsorption as observed in Figs. 2 and 4, with an E_{ads} difference up to 100 kJ/mol between the molecular and dissociative agent-TiO_2 systems. This could suggest that after an initial molecular adsorption of DMMP, Sarin and Soman on TiO_2, a later dissociation of the agent would be expected due to the higher stability of this type of adsorption. Nevertheless, a complementary study of the reaction pathways and the energy barriers would provide additional information to corroborate this assumption. The proposed interaction of DMMP, Sarin and Soman with dry TiO_2(110) are represented in Schemes 1, 2 and 3, respectively. The most favorable interaction of the agents with the TiO_2(110) surface in the gas state, molecular adsorption and dissociative adsorption are represented in States I, II and III, respectively, for each scheme. The dissociative adsorption of Sarin and Soman on metal oxides represents an important method for decontamination of the nerve agents, especially with the dissociation of the fluorophosphate group, obtained in this work as the most stable dissociative adsorption of Sarin and Soman on a dry TiO_2(110) surface, which could lead to a reduction of the products toxicity.

For the agent-TiO_2 system in a dissociative configuration, there are some additional geometrical parameters to consider compared to the molecular adsorption of the molecule. In Fig. 5 and Table 2 the geometric parameters for the most stable agent-TiO_2 in a dissociative configuration are shown. One of the relevant features of the agent-TiO_2 geometric parameters in a dissociative adsorption is the different geometry of the simulant DMMP compared to the agents Sarin and Soman. While in DMMP, the molecule is dissociated into two molecules, in the nerve agents the F atom dissociates causing the rearrangement of the $(CH_3)_xC_yHO_2P$ group with the formation of an additional bond with a O surface atom from TiO_2(110), as observed in Fig. 4. The O−Ti distance between the simulant and the nerve agents have a significant variation especially for the bonds involving the O surface atom from TiO_2(110) in the dissociative products of the nerve agents. The bond formed between the O surface atom, and the nerve agents dissociated molecule generates an elongation of the Ti−O bond between 0.2 and 0.3 nm in order to stabilize the Sarin and Soman dissociative products.

3.2. Effect of water adsorption on the agent-TiO_2 systems

3.2.1. Water adsorption on TiO_2(110)

In most of the previous experimental studies considering the adsorption of agents on metal oxides, the authors reported the presence of H_2O on the metal oxide surface [16,17,20,33,41]. In order to perform a qualitative comparison with previous experimental works, we considered the adsorption of H_2O on the TiO_2(110) surface for the molecular and dissociative adsorption of the agent. The theoretical study of a wet surface requires the consideration of different factors such as the H_2O coverage and the type of H_2O adsorption. According to previous theoretical results, the adsorption of H_2O on TiO_2(110) can be displayed in a molecular(hydrated) or a dissociative(hydroxylated) conformation [54]. The experimental results suggest that at low coverages H_2O does not dissociate on a defect-free TiO_2(110) [55]. The E_{ads} values of H_2O adsorbed on TiO_2(110) with hydrated and hydroxylated conformations predicted by theoretical methods are very similar (difference of around 3 kJ/mol) but the high accuracy of DFT in the calculation of E_{ads} allows us to distinguish between even small energy values and shows that hydrated TiO_2(110) surface is more stable than the

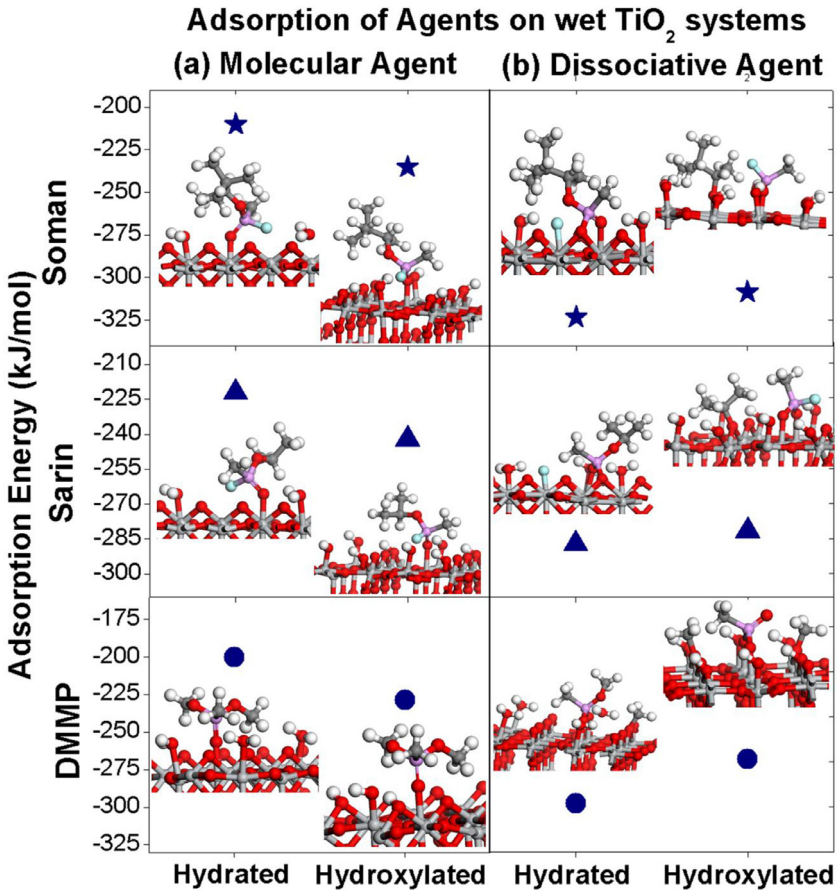

Fig. 6. Adsorption energy in kJ/mol and structure of the agents DMMP (circle), Sarin (triangle) and Soman (star) on a hydrated and hydroxylated TiO_2(110) surface for (a) molecular adsorption and (b) dissociative adsorption of the agent.

hydroxylated one. Using DFT, we calculated the E_{ads} of H_2O on TiO_2(110) with a hydrated and hydroxylated conformation for a 0.5 monolayer coverage obtaining values of −89.7 and −86.7 kJ/mol, respectively. Previous theoretical works obtained values of –73.3 kJ/mol (hydrated) and −67.5 kJ/mol (hydroxylated) for the adsorption of H_2O on TiO_2(110), for the same molecular coverage considered in this study [56,57]. The experimental studies reported E_{ads} between −58.9 and −99.4 kJ/mol, which indicates a good accuracy in our E_{ads} calculations.

3.2.2. Molecular adsorption of DMMP, Sarin and Soman on wet TiO_2(110)

The presence of H_2O on the metal oxide surface is a relevant factor to consider during the adsorption of CWA and simulants. As described in previous sections, the E_{ads} and stability of agent-TiO_2 can show a significant variation with the conformation and structure of the agents. Similarly, factors such as the environmental conditions have shown to modify the E_{ads} in molecules—metal oxide systems, which could be particularly reflected by the presence of water on the surface [58]. In this section, we study the molecular adsorption of the agents on hydrated and hydroxylated TiO_2(110) and calculate the E_{ads} for different possible configuration of the molecularly adsorbed agent on the wet TiO_2 surface (shown in Supporting Information S7–S12)

The E_{ads} for the adsorption of the agents on the wet TiO_2 systems can be calculated with the expression:

$$E_{ads} = E_{Agent-TiO_2(110)-H_2O} - E_{TiO_2(110)-H_2O} - E_{Agent} \quad (2)$$

where $E_{Agent-TiO_2(110)-H_2O}$ is the energy of the agent adsorbed on the wet TiO_2, $E_{TiO_2(110)-H_2O}$ is the energy of the wet TiO_2(110), with H_2O either in a hydrated or hydroxylated conformation and E_{Agent} is the energy of the gas phase isolated agent (DMMP, Sarin or Soman). Fig. 6(a) shows the E_{ads} and final structures for the molecular adsorption of DMMP, Sarin, Soman on the hydrated and hydroxylated TiO_2 surface. The E_{ads} values for the different systems are between −242.2 and −200.0 kJ/mol. The comparison in the E_{ads} values for molecular adsorption of the agents on a hydrated and hydroxylated TiO_2 surface shows that DMMP, Sarin and Soman will show a higher stability for the hydroxylated TiO_2(110) surface. In general, the final structure for DMMP, Sarin and Soman on a wet TiO_2(110) surface is similar to the structures of the dry agent-TiO_2 systems with a bond formed between the P═O group of the agent and the Ti_{5fc} atom of the TiO_2 surface. However, there is an additional interaction between the O of the agents and the H of the H_2O or OH groups adsorbed on TiO_2 that leads to the formation of H bonds. This variation in the final agent-TiO_2 structures is reflected in the E_{ads} variation of the wet systems. In general, the structure of the agents for hydrated and hydroxylated systems are very similar, with the main difference being due to the interaction of the agent with the H_2O or OH groups or the TiO_2 surface.

The comparison in E_{ads} between the dry and wet TiO_2 systems indicates that there is a variation in the E_{ads} between the different agents when adsorbed on TiO_2(110). The DMMP-TiO_2 system had the highest (lowest) E_{ads} among the dry (wet) configurations. Conversely, Sarin-TiO_2 showed the lowest (highest) E_{ads} among the dry (wet) systems.

3.2.3. Dissociative adsorption of DMMP, Sarin and Soman on wet TiO_2(110)

Previously, we described the relevance of the dissociative adsorption of the agents in the decontamination process of CWA. The dissociative adsorption of the nerve agents Sarin and Soman and the simulant DMMP on metal oxide surfaces has been reported primarily under the presence of water in different experimental and theoretical

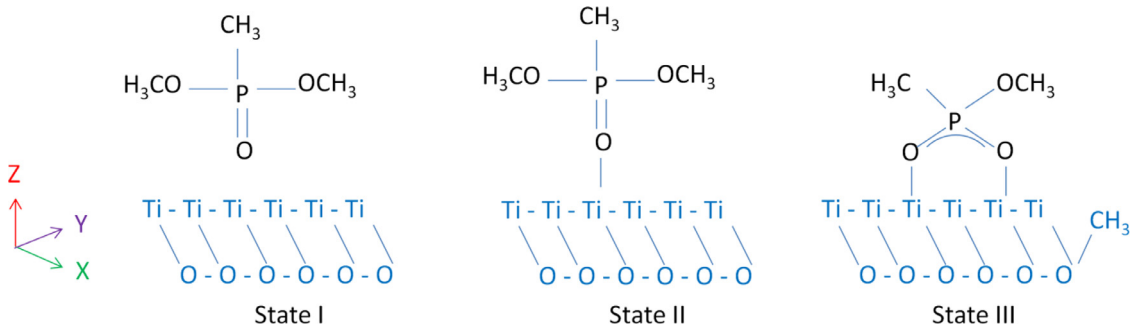

Scheme 1. Adsorption states of DMMP on dry TiO_2(110). (State I) Gas phase, (State II) Molecularly adsorbed, (State III) Dissociatively adsorbed.

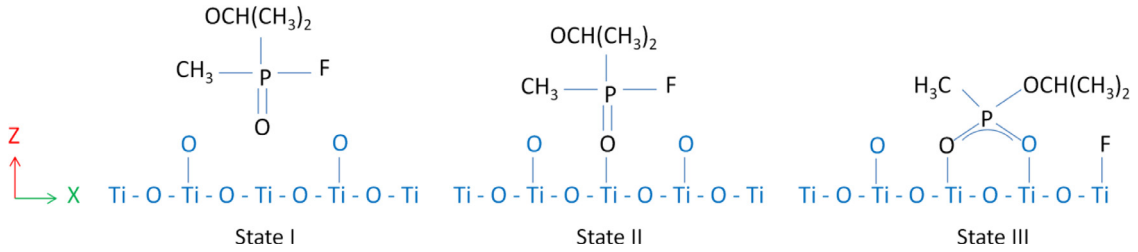

Scheme 2. Adsorption states of Sarin on dry TiO_2(110). (State I) Gas phase, (State II) Molecularly adsorbed, (State III) Dissociatively adsorbed.

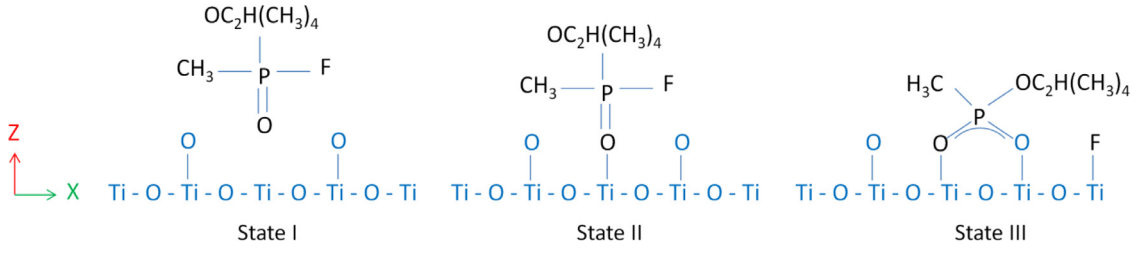

Scheme 3. Adsorption states of Soman on dry TiO_2(110). (State I) Gas phase, (State II) Molecularly adsorbed, (State III) Dissociatively adsorbed.

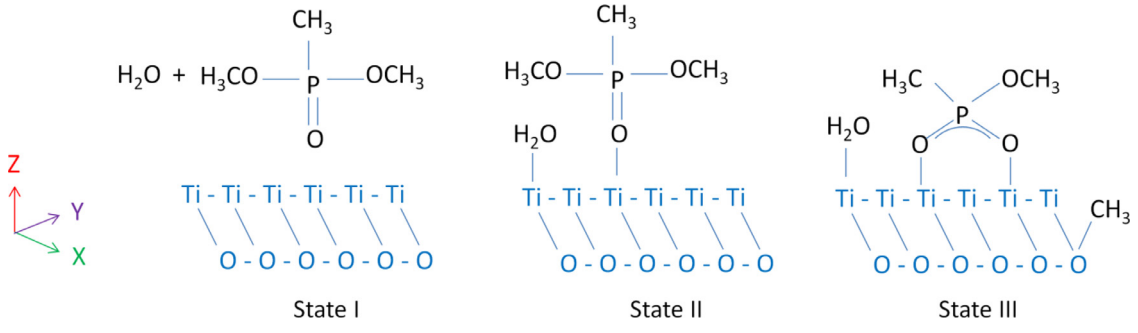

Scheme 4. Adsorption states of DMMP on wet TiO_2(110). (State I) Gas phase, (State II) Molecularly adsorbed, (State III) Dissociatively adsorbed.

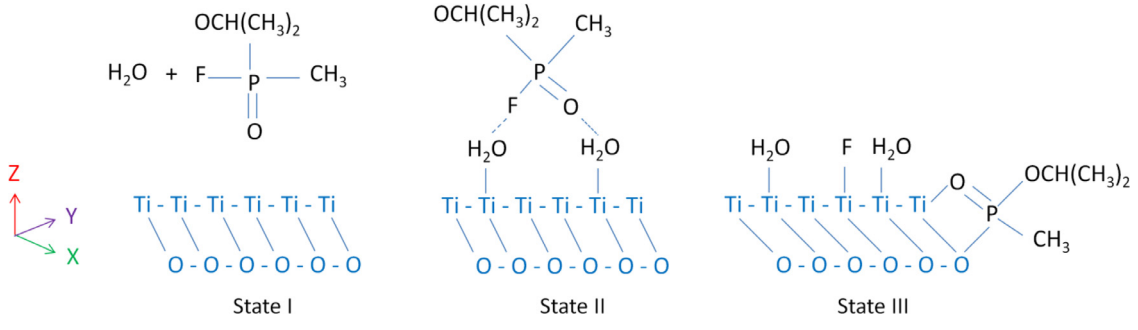

Scheme 5. Adsorption states of Sarin on wet TiO_2(110). (State I) Gas phase, (State II) Molecularly adsorbed, (State III) Dissociatively adsorbed.

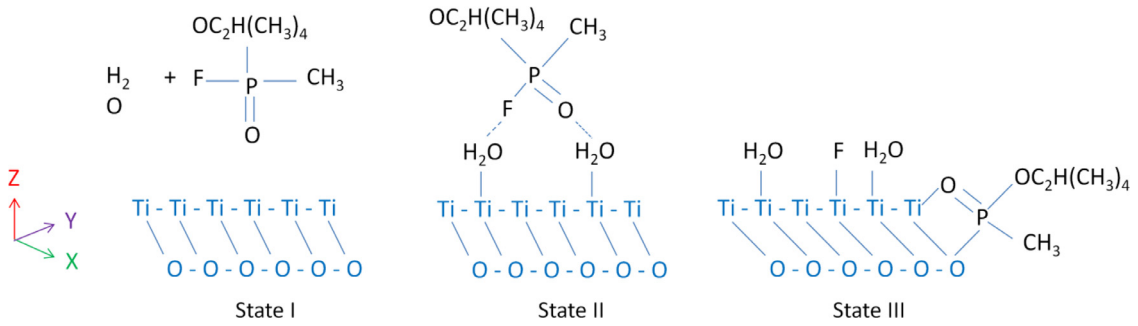

Scheme 6. Adsorption states of Soman on wet TiO_2(110). (State I) Gas phase, (State II) Molecularly adsorbed, (State III) Dissociatively adsorbed.

studies [16,17,20,33,41]. Here, we explore the dissociative adsorption of the agents DMMP, Sarin and Soman on the hydrated and hydroxylated TiO_2(110) surface (with molecular adsorption and dissociative adsorption of H_2O on the TiO_2 surface, respectively). We considered different initial possible dissociative configurations of the agents on the wet TiO_2 surface (shown in Supporting Information S13–S18) and calculated their E_{ads} values.

Fig. 6(b) shows the E_{ads} and final structures of the dissociated agents on a hydrated and hydroxylated TiO_2(110)surface. The E_{ads} for the dissociated agent adsorbed on a wet TiO_2 can be calculated using Eq. (2), with the $E_{Agent-TiO_2(110)-H_2O}$ expression corresponding to the dissociative adsorption of the agent on the wet TiO_2. The E_{ads} values of the dissociative adsorption of the Agents on a wet TiO_2(110) surface are between −323.3 and −268.1 kJ/mol with a preferred configuration for the hydrated systems. The dissociative adsorption of DMMP on hydrated TiO_2 was identified with the dissociation of a methyl groups and its adsorption on the surface with the remaining $(CH_3)_2O_3P$ group forming a bidentate configuration with two Ti_{5fc} surface atoms, similar to the dissociation of the dry systems. The dissociative adsorption of the nerve agents Sarin and Soman on a hydrated TiO_2(the preferred dissociative adsorption) occurs with the dissociation of the F atom and its adsorption on a Ti_{5fc} atom, similarly to dry systems. However, in the hydroxylated TiO_2 surface, Sarin and Soman dissociate in a CH_3FO_2P and a $(CH_3)_vC_wH$ molecule ($v = 2$, $w = 1$ for Sarin and $v = 4$, $w = 2$ for Soman) as observed in Fig. 6(b). These results imply that given the lowest E_{ads} values for the nerve agents on a hydrated TiO_2 surface, the dissociative adsorption of Sarin and Soman through the dissociation of the F atom and its adsorption on the hydrated TiO_2 surface is the final preferred adsorption mechanism for both agents.

The E_{ads} comparison between the molecular and dissociative adsorption of DMMP, Sarin and Soman on a wet TiO_2 surface shows a lower E_{ads} for the dissociative adsorption (between 39.2 and 113.2 kJ/mol) and then higher stability for this configuration, similar to the results observed for the dry systems. In addition, the dissociative adsorption of Sarin and Soman on TiO_2 is more stable in hydrated systems compared to the hydroxylated ones, in contrast to the molecular adsorption of the agents which has shown higher stability for the hydroxylated systems. Therefore, the initial molecular adsorption of the agents on wet TiO_2 and the subsequent dissociation of DMMP, Sarin and Soman on hydrated TiO_2 could be described as the preferred adsorption mechanisms of the agents on wet TiO_2 surfaces, given the comparative lower E_{ads} of these systems. The proposed interaction of DMMP, Sarin and Soman with wet TiO_2(110) are represented in Schemes 4, 5 and 6, respectively. The most favorable interaction of the agents with the TiO_2(110) surface in the gas state, molecular adsorption and dissociative adsorption are represented in States I, II and III, respectively of each scheme.

The comparison between the different models considered in this work shows that the dissociative adsorption of the agents on TiO_2 is more stable than the molecular one for both wet and dry systems. In addition, the agent-TiO_2 systems with wet surfaces were more stable compared to the dry ones for the different configurations considered. In general, the systems that displayed the lowest E_{ads} and then the higher stability among the different configuration were the agent adsorbed on hydrated TiO_2 systems. These results agree with previous experimental studies suggesting the water content to be an important factor in the decontamination process of CWA on TiO_2 materials [59].

4. Comparison with previous studies on the adsorption of agents on TiO_2

Several previous experimental and theoretical studies considered the adsorption of DMMP on TiO_2 while a more limited number focused on the adsorption of the nerve agent Sarin on the same metal oxide [6,7,16,17,20,32–34,41]. There are no previous reports in the literature considering the adsorption of Soman on TiO_2(110), to the best of our knowledge. Experimental studies on the adsorption and thermal decomposition of DMMP on wet TiO_2 showed that both molecular and dissociative adsorption of the simulant on wet TiO_2 can occur [16,17,33]. The dissociative adsorption of DMMP on TiO_2 is described as the initial dissociation of methyl groups and their interaction with a surface oxygen atom to form Ti−OCH_3 and a methyl methylphosphate group with a bidentate configuration, as also proposed in this work and observed in Fig. 6(b) for wet systems. Other experimental works suggested a similar dissociative structure for DMMP on hydroxylated TiO_2 with a further elimination of methanol for temperatures higher than 486 K [14]. We considered similar dissociative structures with methanol elimination as observed in Supporting Information (S16), but our results showed a lower stability for this configuration. In this work, we did not consider the temperature factor in the calculation of the stable configurations for the agent-TiO_2 systems, which could be the reason for the differences in the final dissociative structure predicted for DMMP on hydroxylated TiO_2.

Theoretical studies reported the E_{ads} for molecular adsorption of DMMP and Sarin on wet and dry TiO_2 clusters [34]. The results showed higher stability for the adsorption of the agents on dry TiO_2 clusters compared to the wet ones at full monolayer coverage. However, in this particular H_2O coverage the dissociation and further interaction of the molecule with the surface could be limited due to the pervasive presence of H_2O in a hydrated and hydroxylated configurations. A similar study on the adsorption of DMMP on rutile TiO_2(110) compared the E_{ads} between the slab and the cluster models [6]. The DMMP-TiO_2 E_{ads} values for a slab system, a large cluster and a small cluster where −184.3, −130.3, −103.2 kJ/mol, respectively. This paper emphasized the significant difference in the E_{ads} between slab and cluster systems and how the selection of the adequate size of the cluster is imperative in order to obtain reliable E_{ads} values that can be comparable to the slab configurations. Other theoretical studies on the adsorption of DMMP on TiO_2 anatase clusters, reported a preferred dissociative adsorption on wet TiO_2 [32], with higher stability for the hydrated systems compared to the hydroxylated ones, as also observed in the present work. The theoretical E_{ads} of DMMP on dry TiO_2(110) was also calculated for slab surfaces for the molecular and dissociative adsorption of DMMP [7]. The dissociative adsorption of the molecule was obtained as the most

preferred configuration, with the CH_3 dissociative product adsorbing on a surface oxygen atom, similar to the dissociative configuration obtained in this work and shown in Fig. 4. Nevertheless, the E_{ads} values obtained in the present study and the ones reported by Bermudez [7] (−73.3 and −108.1 kJ/mol for molecular and dissociative adsorption of DMMP on TiO_2, respectively) are significantly different which may be due to the variation in the methods and theory level employed. Bermudez used the restricted Hartree–Fock level of theory for geometry optimization of the slab systems and the B3YLP functional for a single point calculation of the total energies. Also the van der Waals interactions were not included in the energy calculations, which could have generated differences in the final geometry and the final energy calculations of the systems in comparison to the present study.

Previous experimental studies also considered the photocatalytic decomposition of Sarin on TiO_2 [20,41]. The dissociated products of Sarin on a hydroxylated TiO_2 surface were similar to the ones obtained here, with the F atom dissociating from the nerve agents and adsorbing on the hydroxylated metal oxide surface, as observed in Fig. 6(b). A theoretical work in the reaction mechanism of Sarin Hydrolysis with $Cs_8Nb_6O_{19}$ showed that the presence of water can assist the elimination of isopropanol [60]. We explored similar dissociative products with alcohol elimination from Sarin and Soman on hydroxylated TiO_2. The dissociative products $(CH_3)_2CHOH$ and $(CH_3)_4C_2HOH$ from Sarin and Soman, respectively, with the CH_3PO_2F group adsorbed on the TiO_2(110) surface were considered as observed in Supporting Information (S17 and S18). Our results show that these dissociative products have higher E_{ads} and then are less thermodynamically stable compared with the dissociation of F from Sarin and Soman.

Considering the previous theoretical and experimental works reported here on the adsorption of agents on wet and dry TiO_2, the dissociative adsorption of DMMP and Sarin on this metal oxide was identified as the preferred adsorption mechanism.

5. Conclusions

The adsorption energy and geometry of DMMP, Sarin and Soman on TiO_2(110) under dry and wet conditions were investigated using density functional theory. We found that the dissociative adsorption of the simulant and agents in the hydrated TiO_2(110) had the lowest adsorption energy and thus the higher stability among the different systems considered. In addition, the dissociative adsorption of the agents on TiO_2 was more stable than the molecular adsorption for both wet and dry systems. This result is in agreement with the experimental studies that show the adsorption of H_2O on TiO_2 being an important factor in the dissociative adsorption of the agents. In terms of the final geometries, the final dissociative structure in the dry and hydrated nerve agent-TiO_2 systems was observed to be that with the F atom dissociating from Sarin and Soman and forming a bond with a Ti surface atom. Also, the difference in the dissociative structures for the agent-TiO_2 systems with H_2O in a hydrated and hydroxylated configurations suggests that not only the water content but also the configuration of the molecules affect the stability and structure of the agents adsorbed on TiO_2. The comparison in the dissociation process between the agents Sarin and Soman, and the simulant DMMP on TiO_2 showed that for the agents, as well as the simulant, the dissociation under hydrated conditions is preferred, although the dissociative mechanism and products for DMMP on TiO_2(110) have a significant variation from those for the agents Sarin and Soman. A future study focused on the energy barrier calculations for the final geometries obtained here could provide additional understanding of the energy path for the dissociation of the agent-TiO_2 systems. Similar theoretical studies can be extended to other toxic agents to determine the preferred adsorption mechanisms and structures on different surfaces.

Acknowledgments

The research was supported by Natick Soldier Research, Development & Engineering Center. Yenny Cardona Quintero acknowledges the support from the National Research Council Postdoctoral Fellowship program. Computational support through the DOD High-Performance Computing Modernization Program is also gratefully acknowledged.

Supplementary materials

Supplementary material associated with this article can be found, in the online version, at doi:10.1016/j.susc.2018.04.002.

References

[1] N. Sharma, R. Kakkar, Recent advancements on warfare agents/metal oxides surface chemistry and their simulation study, Adv. Mat. Lett. 4 (2013) 508–521.
[2] Y.J. Jang, K. Kim, O.G. Tsay, D.A. Atwood, D.G. Churchill, Update 1 of: destruction and detection of chemical warfare agents, Chem. Rev. 115 (2011) PR1–PR76.
[3] V. Štengl, J. Henych, P. Janoš, M. Skoumal, Nanostructured metal oxides for stoichiometric degradation of chemical warfare agents, Rev. Environ. Contam. Toxicol. 236 (2016) 239–258.
[4] D. Majumdar, S. Roszak, J. Wang, T.C. Dinadayalane, B. Rasulev, H. Pinto, J. Leszczynski, Advances in in silico research on nerve agents, Practical Aspects of Computational Chemistry III (2014) 283–322.
[5] R. Black, Development, historical use and properties of chemical warfare agents, Chemical Warfare Toxicology: Volume 1: Fundamental Aspects 1 The Royal Society of Chemistry, 2016, pp. 1–28.
[6] L. Yang, D. Tunega, L. Xu, N. Govind, R. Sun, R. Taylor, H. Lischka, W.A. Dejong, W.L. Hase, Comparison of cluster, slab, and analytic potential models for the dimethyl methylphosphonate (DMMP)/TiO_2(110) intermolecular interaction, J. Phys. Chem. C 117 (2013) 17613–17622.
[7] V.M. Bermudez, Ab initio study of the interaction of dimethyl methylphosphonate with rutile (110) and anatase (101) TiO_2 surfaces, J. Phys. Chem. C 114 (2010) 3063–3074.
[8] V.M. Bermudez, Computational study of environmental effects in the adsorption of DMMP, Sarin, and VX on γ-Al_2O_3: photolysis and surface hydroxylation, J. Phys. Chem. C 113 (2009) 1917–1930.
[9] V.M. Bermudez, First-principles study of adsorption of dimethyl methylphosphonate on the TiO_2 anatase (001) surface: formation of a stable titanyl (Ti=O) site, J. Phys. Chem. C 115 (2011) 6741–6747.
[10] V.M. Bermudez, Computational study of the adsorption of dimethyl methylphosphonate (DMMP) on the (010) surface of anatase TiO_2 with and without faceting, Surf. Sci. 604 (2010) 706–712.
[11] A. Michalkova, M. Ilchenko, L. Gorb, J. Leszczynski, Theoretical study of the adsorption and decomposition of sarin on magnesium oxide, J. Phys. Chem. B 108 (2004) 5294–5303.
[12] A. Michalkova, J. Leszczynski, Interactions of nerve agents with model surfaces: computational approach, J. Vac. Sci. Technol. A 28 (2010) 1010–1017.
[13] B.N. Papas, I.D. Petsalakis, G. Theodorakopoulos, J.L. Whitten, CI and DFT studies of the adsorption of the nerve agent sarin on surfaces, J. Phys. Chem. C 118 (2014) 23042–23048.
[14] C.N. Rusu, J.T. Yates, Adsorption and decomposition of dimethyl methylphosphonate on TiO_2, J. Phys. Chem. B 104 (2000) 12292–12298.
[15] E. Durke Davis, W.O. Gordon, A.R. Wilmsmeyer, D. Troya, J.R. Morris, Chemical warfare agent surface adsorption: hydrogen bonding of sarin and soman to amorphous silica, J. Phys. Chem. Lett. 5 (2014) 1393–1399.
[16] D.A. Panayotov, J.R. Morris, Uptake of a chemical warfare agent simulant (DMMP) on TiO_2: reactive adsorption and active site poisoning, Langmuir 25 (2009) 3652–3658.
[17] D.A. Panayotov, J.R. Morris, Thermal decomposition of a chemical warfare agent simulant (DMMP) on TiO_2: adsorbate reactions with lattice oxygen as studied by infrared spectroscopy, J. Phys. Chem. C 113 (2009) 15684–15691.
[18] J. Zhou, S. Ma, Y.C. Kang, D.A. Chen, Dimethyl methylphosphonate decomposition on titania-supported ni clusters and films: a comparison of chemical activity on different Ni surfaces, J. Phys. Chem. B 108 (2004) 11633–11644.
[19] J. Zhou, K. Varazo, J.E. Reddic, M.L. Myrick, D.A. Chen, Decomposition of dimethyl methylphosphonate on TiO_2 (110): principal component analysis applied to x-ray photoelectron spectroscopy, Anal. Chem. Acta 496 (2003) 289–300.
[20] K. Sato, T. Hirakawa, A. Komano, S. Kishi, C.K. Nishimoto, N. Mera, M. Kugishima, T. Sano, H. Ichinose, N. Negishi, et al., Titanium dioxide photocatalysis to decompose isopropyl methylphosphonofluoridate (GB) in gas phase, Appl. Catal. B Environ. 106 (2011) 316–322.
[21] P. Janos, J. Henych, O. Pelant, V. Pilarova, L. Vrtoch, M. Kormunda, K. Mazanec, V. Stengl, Cerium oxide for the destruction of chemical warfare agents: a comparison of synthetic routes, J. Hazard. Mater 304 (2016) 259–268.
[22] P. Janos, P. Kuran, M. Kormunda, V. Stengl, T. Matys Grygar, M. Dosek, M. Stastny, J. Ederer, V. Pilarova, L. Vrtoch, Cerium dioxide as a new reactive sorbent for fast degradation of parathion methyl and some other organophosphates, J. Rare Hear. 32 (2014) 360–370.

[23] V.S. Vaiss, I. Borges, A.A. Leit, Sarin degradation using brucite, J. Phys. Chem. C 115 (2011) 24937–24944.
[24] A.R. Wilmsmeyer, W.O. Gordon, E. Durke Davis, D. Troya, B.A. Mantooth, T.A. Lalain, J.R. Morris, Infrared spectra and binding energies of chemical warfare nerve agent simulants on the surface of amorphous silica, J. Phys. Chem. C. 117 (2013) 15685–15697.
[25] A. Michalkova, J. Martinez, O.A. Zhikol, L. Gorb, O.V. Shishkin, D. Leszczynska, J. Leszczynski, Theoretical study of adsorption of sarin and soman on tetrahedral edge clay mineral fragments, J. Phys. Chem. B 110 (2006) 21175–21183.
[26] Y. Paukku, A. Michalkova, J. Leszczynski, Adsorption of dimethyl methylphosphonate and trimethyl phosphate on calcium oxide: an ab initio study, Struct. Chem. 19 (2008) 307–320.
[27] J. Quenneville, R.S. Taylor, A.C.T. van Duin, Reactive molecular dynamics studies of dmmp adsorption and reactivity on amorphous silica surfaces, J. Phys. Chem. C 114 (2010) 18894–18902.
[28] M.R. Housaindokht, N. Zamand, A DFT study of associative and dissociative chemical adsorption of DMMP onto SnO_2(110) surface nano-cluster, Struct. Chem. 26 (2015) 87–96.
[29] A. Michalkova, Y. Paukku, D. Majumdar, J. Leszczynski, Theoretical study of adsorption of tabun on calcium oxide clusters, Chem. Phys. Lett. 438 (2007) 72–77.
[30] I.N. Martyanov, K.J. Klabunde, Photocatalytic oxidation of gaseous 2-chloroethyl ethyl sulfide over TiO_2, Environ. Sci. Technol. 37 (2003) 3448–3453.
[31] G.K. Prasad, B. Singh, K. Ganesan, A. Batra, T. Kumeria, P.K. Gutch, R. Vijayaraghavan, Modified titania nanotubes for decontamination of sulphur mustard, J. Hazard. Mater. 167 (2009) 1192–1197.
[32] D.A. Trubitsyn, A.V. Vorontsov, Molecular and reactive adsorption of dimethyl methylphosphonate over (001) and (100) anatase clusters, Comput. Theor. Chem. 1020 (2013) 63–71.
[33] A. Kiselev, A. Mattson, M. Andersson, A.E.C. Palmqvist, L. Osterlund, Adsorption and photocatalytic degradation of diisopropyl fluorophosphate and dimethyl methylphosphonate over dry and wet rutile TiO_2, J. Photochem. Photobiol. A Chem. 184 (2006) 125–134.
[34] R.S. Taylor, C. Cuiang, R.M. Shroll, Determing the reactivity of CWA on metal oxide surfaces via computational chemistry, Proceeding of Chemical and Biological Defense Physical Science and Technology Conference, New Orleans, LA, 2008.
[35] G.W. Wagner, O.B. Koper, E. Lucas, S. Decker, K.J. Klabunde, Reactions of VX, GD, and HD with nanosize CaO: autocatalytic dehydrohalogenation of HD, J. Phys. Chem. C 104 (2000) 5118–5123.
[36] M.B. Mitchell, V.N. Sheinker, E.A. Mintz, Adsorption and decomposition of dimethyl methylphosphonate on metal oxides, J. Phys. Chem. B 101 (1997) 11192–11203.
[37] A.R. Head, R. Tsyshevsky, L. Trotochaud, Y. Yu, L. Kyhl, O. Karslıoğlu, M.M. Kuklja, H. Bluhm, Adsorption of dimethyl methylphosphonate on MoO_3: the role of oxygen vacancies, J. Phys. Chem. C 120 (2016) 29077–29088.
[38] L. Trotochaud, R. Tsyshevsky, S. Holdren, K. Fears, A.R. Head, Y. Yu, S. Pletincx, B. Eichhorn, M. Zachariah, M.M. Kuklja, et al., Spectroscopic and computational investigation of room-temperature decomposition of a chemical warfare agent simulant on polycrystalline cupric oxide, Chem. Mater. 29 (2017) 7483–7496.
[39] I.V Schweigert, D. Gunlycke, Hydrolysis of dimethyl methylphosphonate by the cyclic tetramer of zirconium hydroxide, J. Phys. Chem. A 121 (2017) 7690–7696.
[40] G. Wang, C. Sharp, A.M. Plonka, Q. Wang, A.I. Frenkel, W. Guo, C. Hill, C. Smith, J. Kollar, D. Troya, et al., Mechanism and kinetics for reaction of the chemical warfare agent simulant, DMMP(g), with zirconium (IV) MOFs: an ultrahigh-vacuum and DFT study, J. Phys. Chem. C 121 (2017) 11261–11272.
[41] T. Hirakawa, K. Sato, A. Komano, S. Kishi, C.K. Nishimoto, N. Mera, M. Kugishima, T. Sano, H. Ichinose, N. Negishi, et al., Experimental study on adsorption and photocatalytic decomposition of isopropyl methylphosphonofluoridate at surface of TiO_2 photocatalyst, J. Phys. Chem. C 114 (2010) 2305–2314.
[42] P. Giannozzi, S. Baroni, N. Bonini, M. Calandra, R. Car, C. Cavazzoni, D. Ceresoli, G.L. Chiarotti, M. Cococcioni, I. Dabo, et al., QUANTUM ESPRESSO: a modular and open-source software project for quantum simulations of materials, J. Phys. Condens. Matter 21 (2009). 395502(1)–395502(36).
[43] J. Perdew, J. Chevary, S. Vosko, K. Jackson, M. Pederson, D. Singh, C. Fiolhais, Atoms, molecules, solids, and surfaces: applications of the generalized gradient approximation for exchange and correlation, Phys. Rev. B 46 (1992) 6671–6687.
[44] P.E. Blöchl, Projector augmented-wave method, Phys. Rev. B 50 (1994) 17953–17979.
[45] S. Grimme, Semiempirical GGA-type density functional constructed with a long-range dispersion correction, J. Compt. Chem. 27 (2006) 1787–1799.
[46] J. Ireta, J. Neugebauer, M. Scheffler, On the accuracy of DFT for describing hydrogen bonds: dependence on the bond directionality, J. Phys. Chem. A 108 (2004) 5692–5698.
[47] C.J. Howard, T.M. Sabine, F. Dickson, Structural and thermal parameters for rutile and anatase, Acta Cryst. B47 (1991) 462–468.
[48] A.R. Head, R. Tsyshevsky, L. Trotochaud, B. Eichhorn, M.M. Kuklja, H. Bluhm, Electron spectroscopy and computational studies of dimethyl methylphosphonate, J. Phys. Chem. A 120 (2016) 1985–1991.
[49] A. Kaczmarek, L. Gorb, A.J. Sadlej, J. Leszczynski, Sarin and soman: structure and properties, Struct. Chem. 15 (2004) 517–525.
[50] T. Ash, T. Debnath, T. Banu, A.K. Das, Exploration of unimolecular gas-phase detoxication pathways of sarin and soman: a computational study from the perspective of reaction energetics and kinetics, Chem. Res. Toxicol. 29 (2016) 1439–1457.
[51] A.V Bandura, J.D. Kubicki, Derivation of force field parameters for TiO_2-H_2O systems from ab initio calculations, J. Phys. Chem. B 107 (2003) 11072–11081.
[52] P.M. Kowalski, B. Meyer, D. Marx, Composition, structure, and stability of the rutile TiO_2(110) surface: oxygen depletion, hydroxylation, hydrogen migration, and water adsorption, Phys. Rev. B 79 (2009). 115410(1)–115410(16).
[53] D. Brinkley, M. Dietrich, T. Engel, P. Farrall, G. Gantner, A. Schafer, A. Szuchmacher, A modulated molecular beam study of the extent of H_2O dissociation on TiO_2(110), Surf. Sci. 395 (1998) 292–306.
[54] P.J.D. Lindan, C. Zhang, Exothermic water dissociation on the rutile TiO_2(110) surface, Phys. Rev. B 72 (2005). 075439(1)–075439(7).
[55] M.A. Henderson, An HREELS and TPD study of water on TiO_2(110): the extent of molecular versus dissociative adsorption, Surf. Sci. 355 (1996) 151–166.
[56] S.C. Smith, C. Sun, L. Liu, A. Selloni, Q. Max, S.C. Smith, Titania-water interactions: a review of theoretical studies, J. Mater. Chem. 20 (2010) 10319–10334.
[57] J. Cheng, M. Sprik, Acidity of the aqueous rutile TiO_2(110) surface from density functional theory based molecular dynamics, J. Chem. Theory Comput. 6 (2010) 880–889.
[58] Y. Cardona Quintero, G. Ramanath, R. Ramprasad, Environment-dependent interfacial strength using first principles thermodynamics: the example of the Pt-HfO_2 interface, J. Appl. Phys. 114 (2013). 163503(1)–163503(4).
[59] G.W. Wagner, G.W. Peterson, J.J. Mahle, Effect of adsorbed water and surface hydroxyls on the hydrolysis of VX, GD, and HD on titania materials: the development of self-decontaminating paints, Ind. Eng. Chem. Res. 51 (9) (2012) 3598–3603.
[60] R.C. Chapleski, D.G. Musaev, C.L. Hill, D. Troya, Reaction mechanism of nerve-agent hydrolysis with the $Cs_8Nb_6O_{19}$ Lindqvist hexaniobate catalyst, J. Phys. Chem. C 120 (2016) 16822–16830.

Supporting Information

Molecular and dissociative adsorption of DMMP, Sarin and Soman on dry and wet TiO_2(110) using density functional theory

Yenny Cardona Quintero, Ramanathan Nagarajan*

Natick Soldier Research, Development & Engineering Center

Natick, MA 01760

Table of Contents

Modeling Details

The adsorption of the agents DMMP, Sarin and Soman on TiO_2(110) rutile were modeled using density functional theory. The agent-TiO_2 systems were built with 1 molecule per 8 Ti atoms 5 fold coordinated (Ti_{5fc}), with a surface area of (2 x 4), five TiO_2 layers (Figure 1a), and a total of 80 TiO_2 groups. The agents were placed on top of TiO_2(110) creating an asymmetric slab which requires the dipole correction to account for the artificial field in the system due to the periodicity of the lattice. A minimum vacuum region of 12 Å was selected after testing its ability to avoid interactions of the molecule with adjacent periodic images. Different possible adsorption configurations of the molecule on the dry TiO_2(110) slab were included as shown below (S1 – S6).

Agent-TiO_2 systems under wet conditions were built to determine the effect of H_2O on the adsorption of agents on the TiO_2(110) surface. The adsorption of H_2O on TiO_2(110) was considered with both a hydrated and hydroxylated configuration with a coverage of 0.5 H_2O monolayer. In the hydrated surface, the H_2O molecules were adsorbed on the top TiO_2 layer forming a bond with the Ti_{5fc} surface atoms. In the hydroxylated configuration, H_2O was dissociated into OH and H, the OH groups were adsorbed on the Ti surface atoms while the H atoms adsorbed on the adjacent O surface atoms. The information from previous experimental and theoretical studies was used to construct and model the TiO_2-H_2O interface. The adsorption of DMMP, Sarin and Soman on the wet TiO_2(110) surface was modeled using the same slab systems described for dry configurations. The initial agent-TiO_2 structures of the wet systems are shown below (S7 – S18).

The selection of the configuration was based on the possible arrangements of the agent on the TiO_2(110) surface including distance to the surface, bond lengths, bond angles, possible secondary bonds formed and orientation of the molecule respect to the surface. Additional initial configurations of the agents on the TiO_2(110) surface were also constructed in based on the geometry reported in previous works as stable systems.

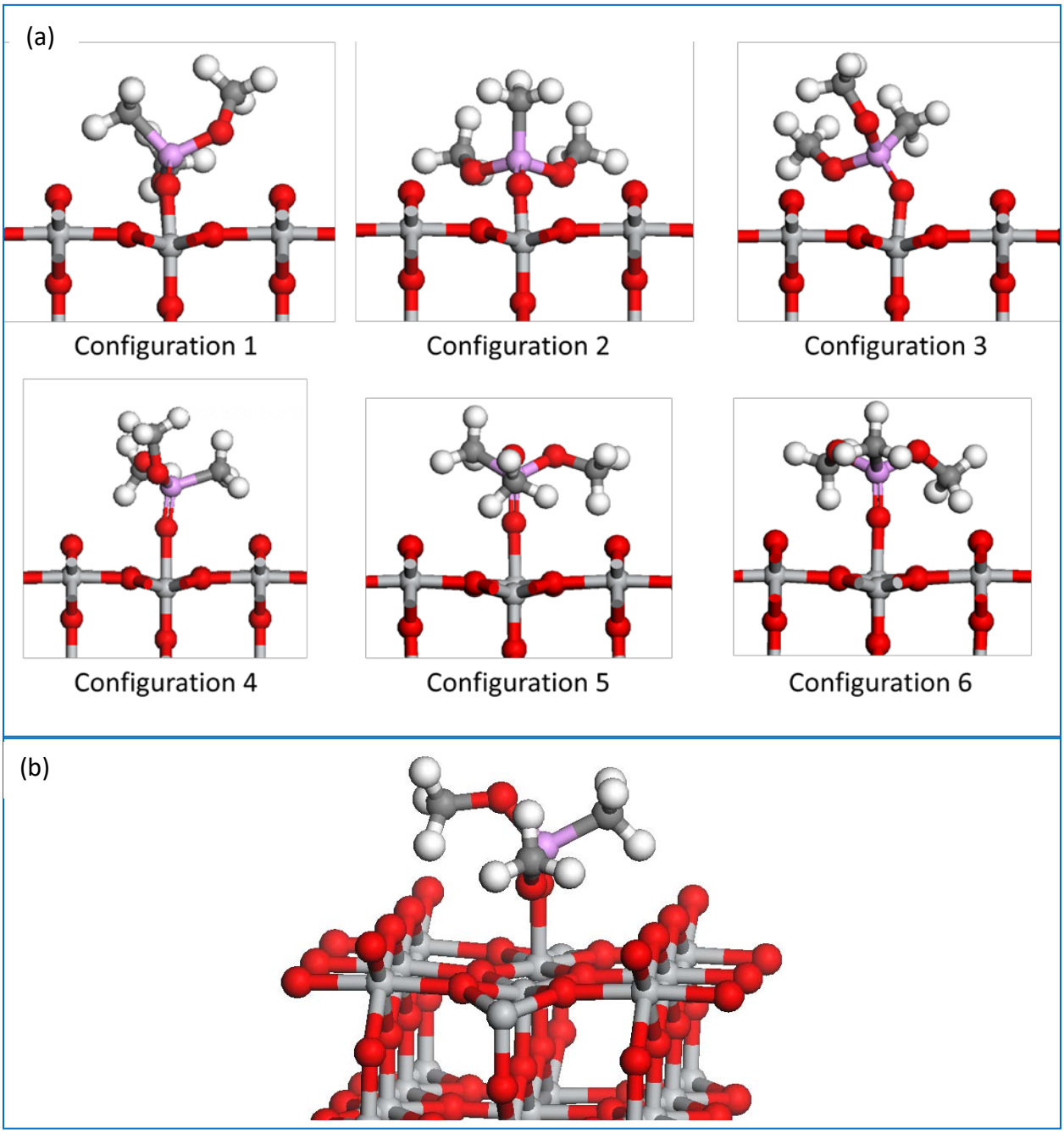

(S1) Molecular adsorption of DMMP on dry TiO_2(110) (a) Initial configurations (b) Final most stable configuration

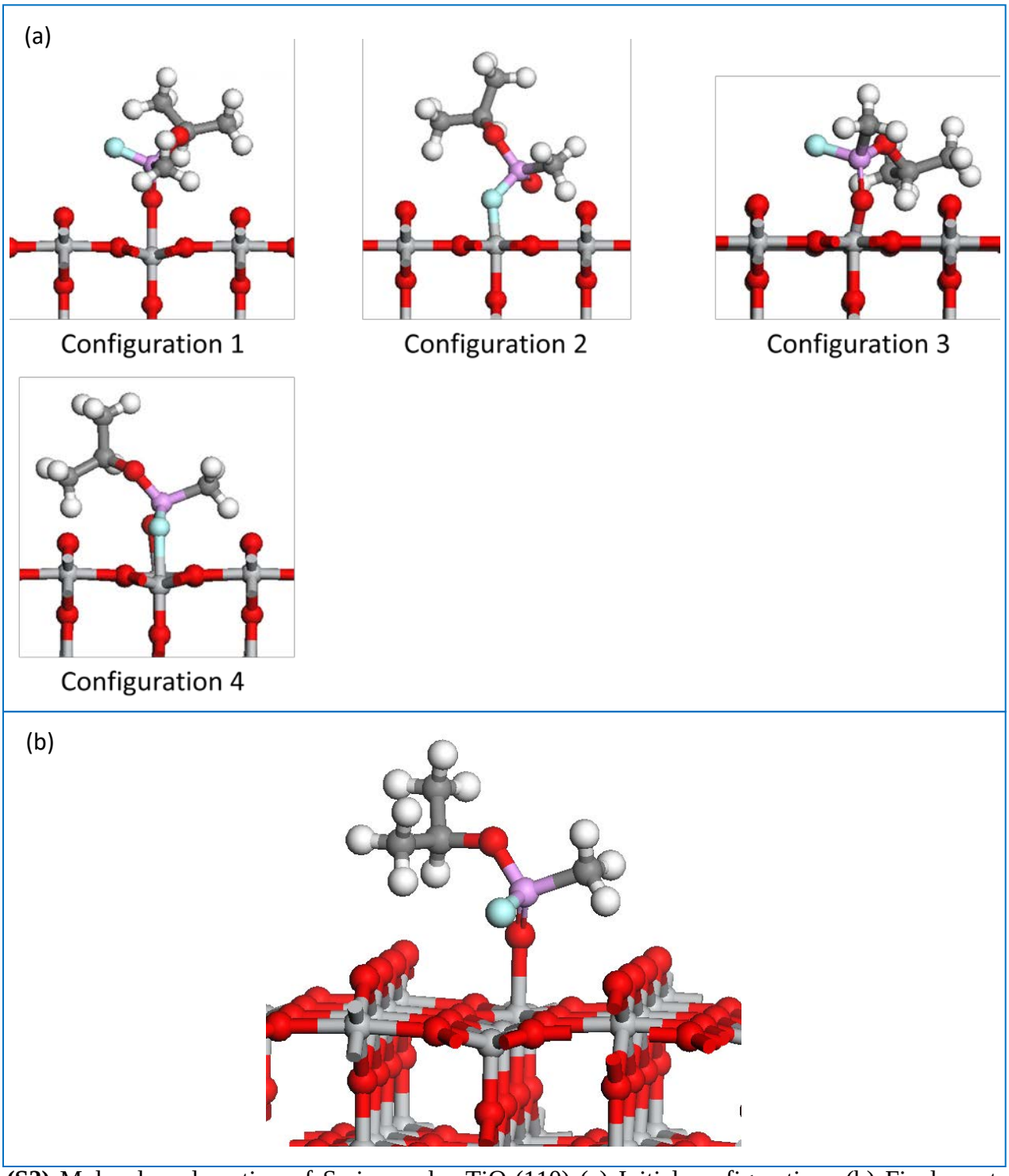

(S2) Molecular adsorption of Sarin on dry TiO_2(110) (a) Initial configurations (b) Final most stable configuration

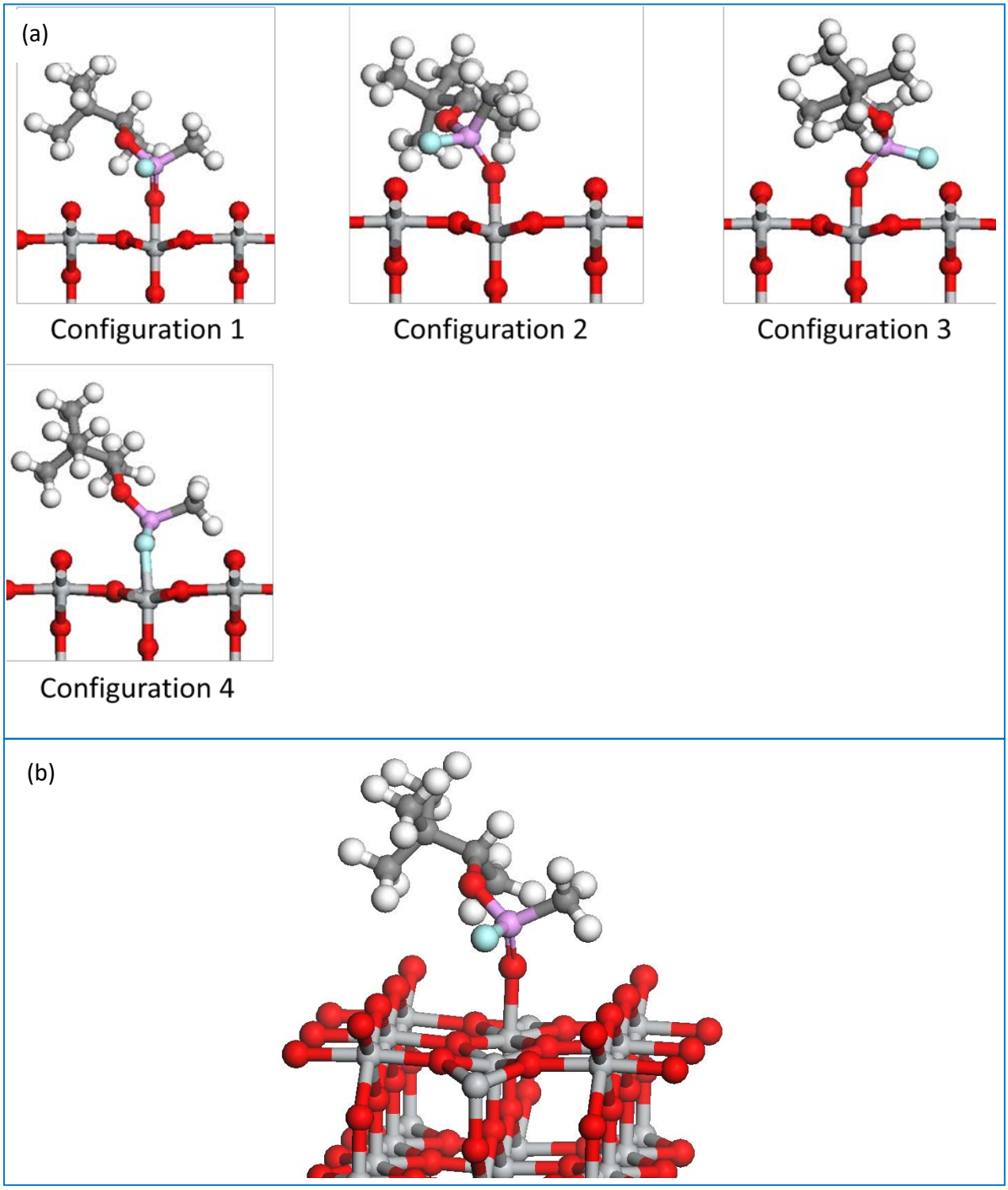

(S3) Molecular adsorption of Soman on dry TiO_2(110) (a) Initial configurations (b) Final most stable configuration

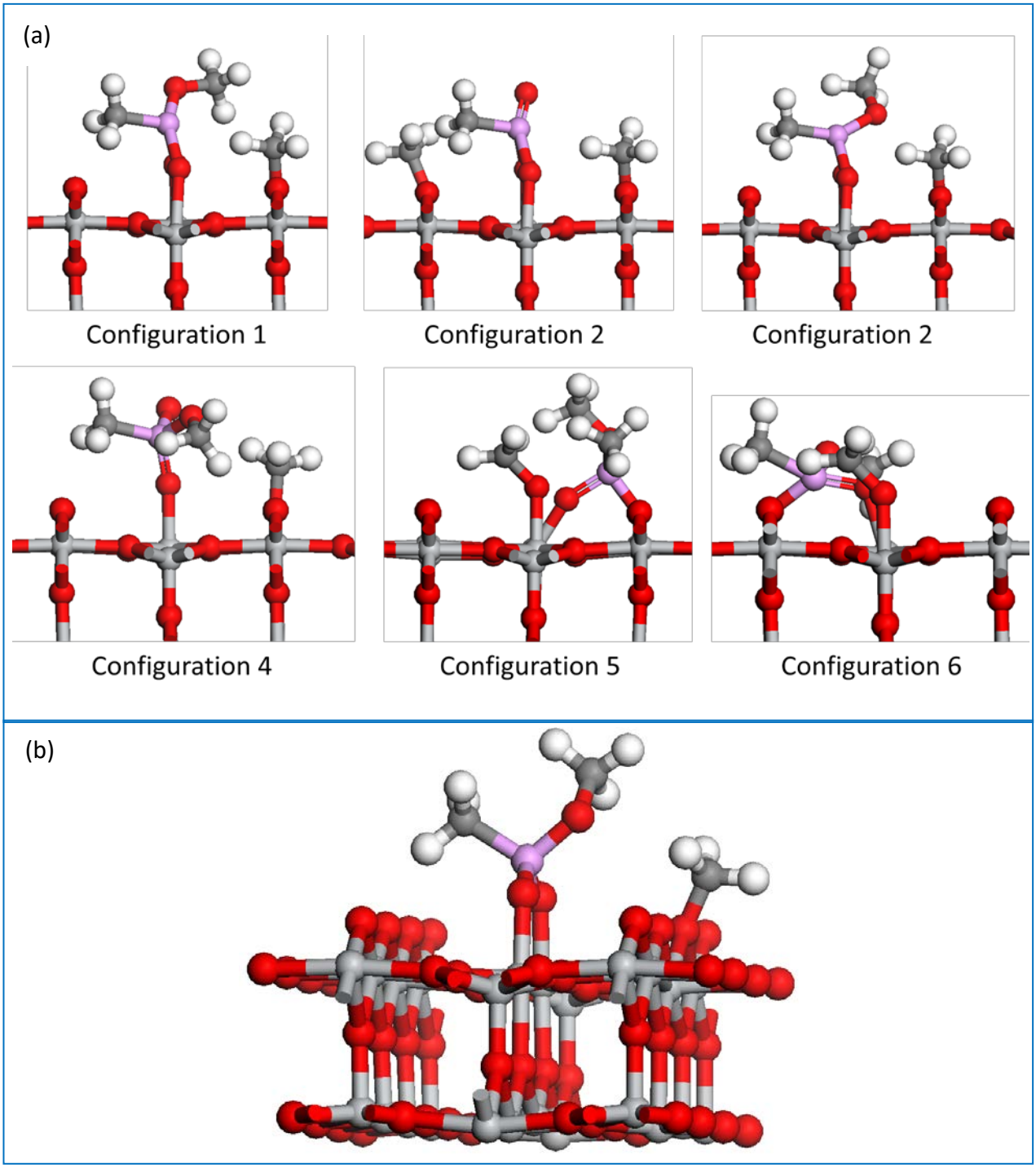

(S4) Dissociative adsorption of DMMP on dry TiO_2(110) (a) Initial configurations (b) Final most stable configuration

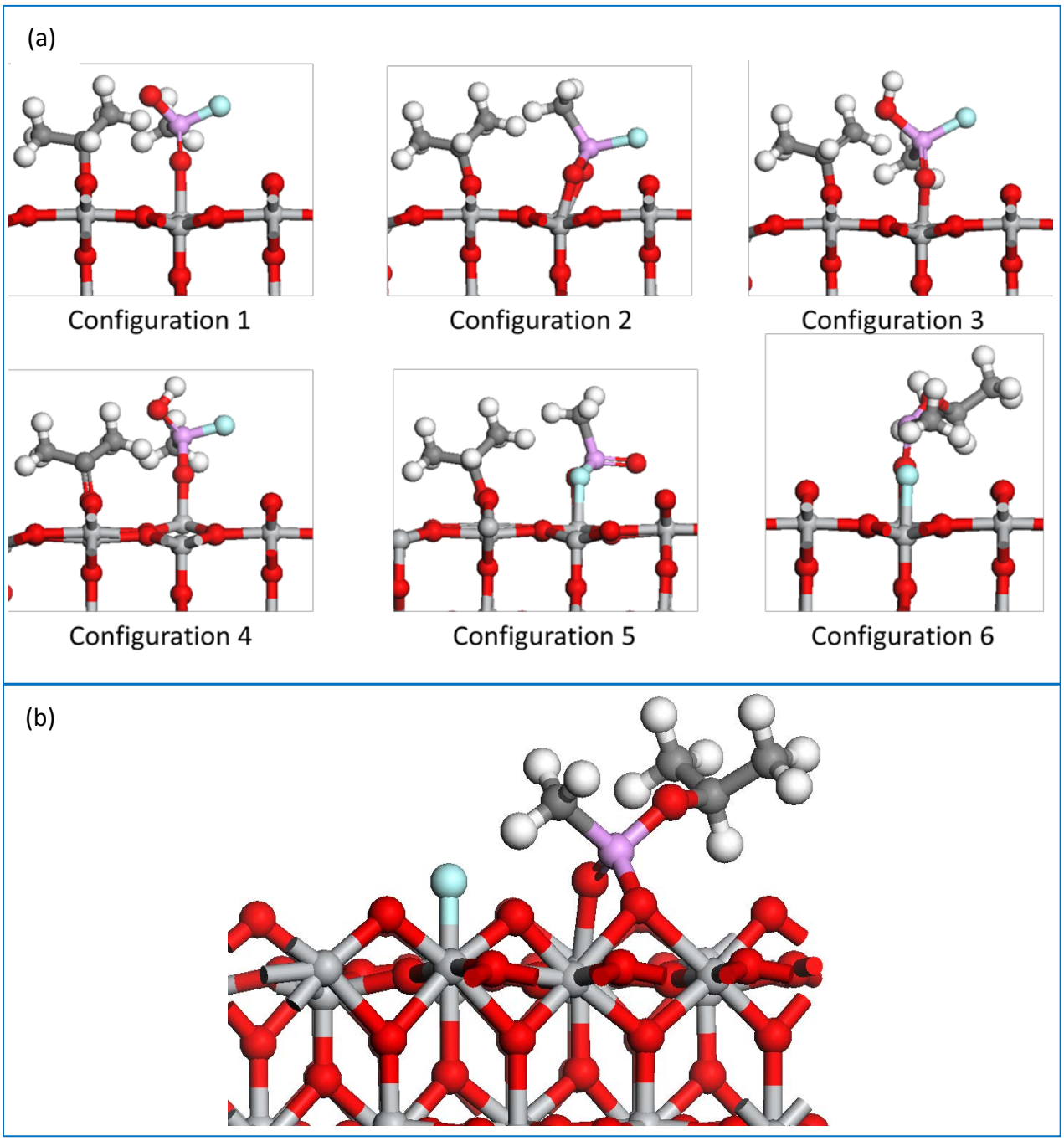

(S5) Dissociative adsorption of Sarin on dry TiO_2(110) (a) Initial configurations (b) Final most stable configuration

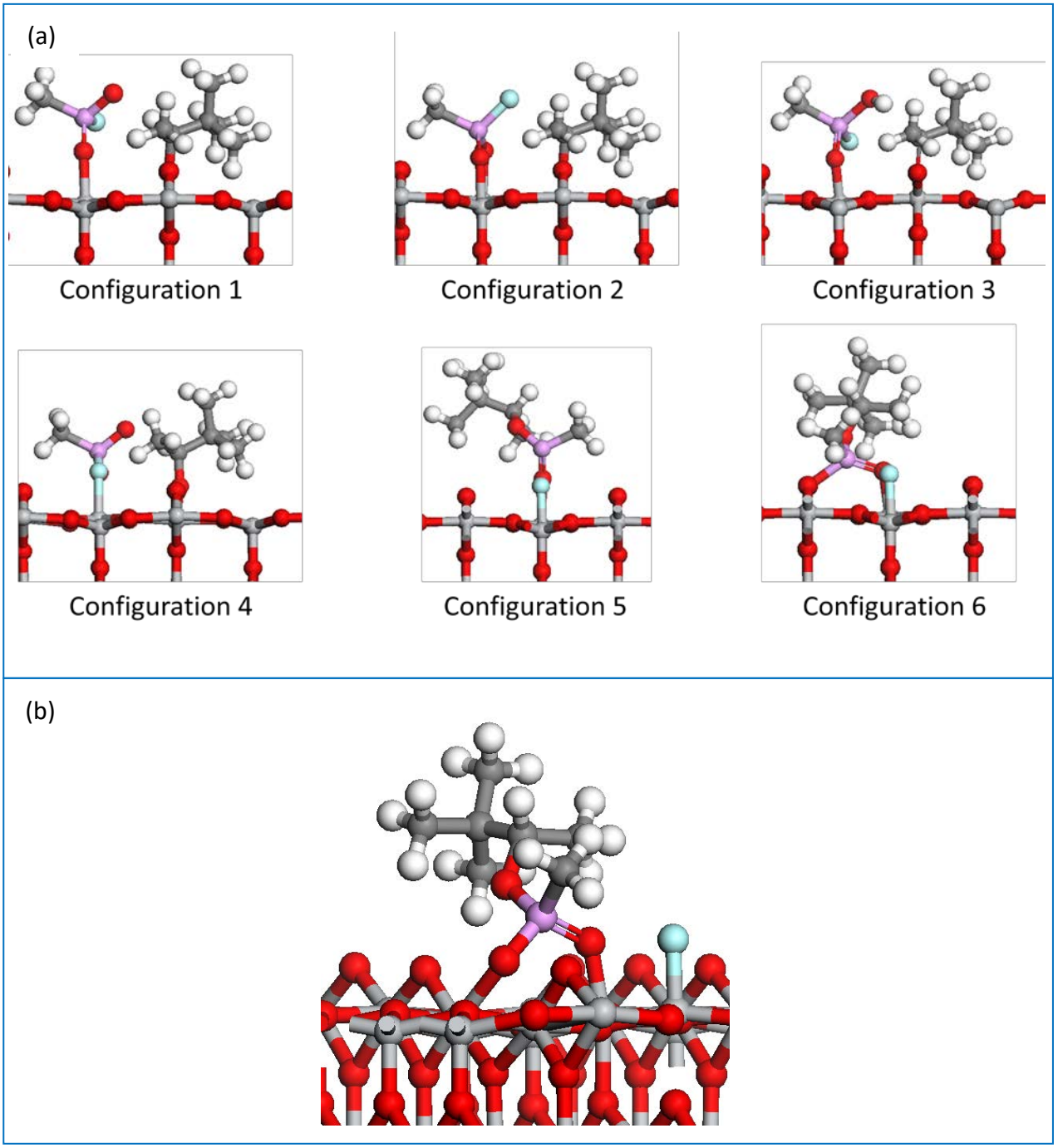

(S6) Dissociative adsorption of Soman on dry TiO_2(110) (a) Initial configurations (b) Final most stable configuration

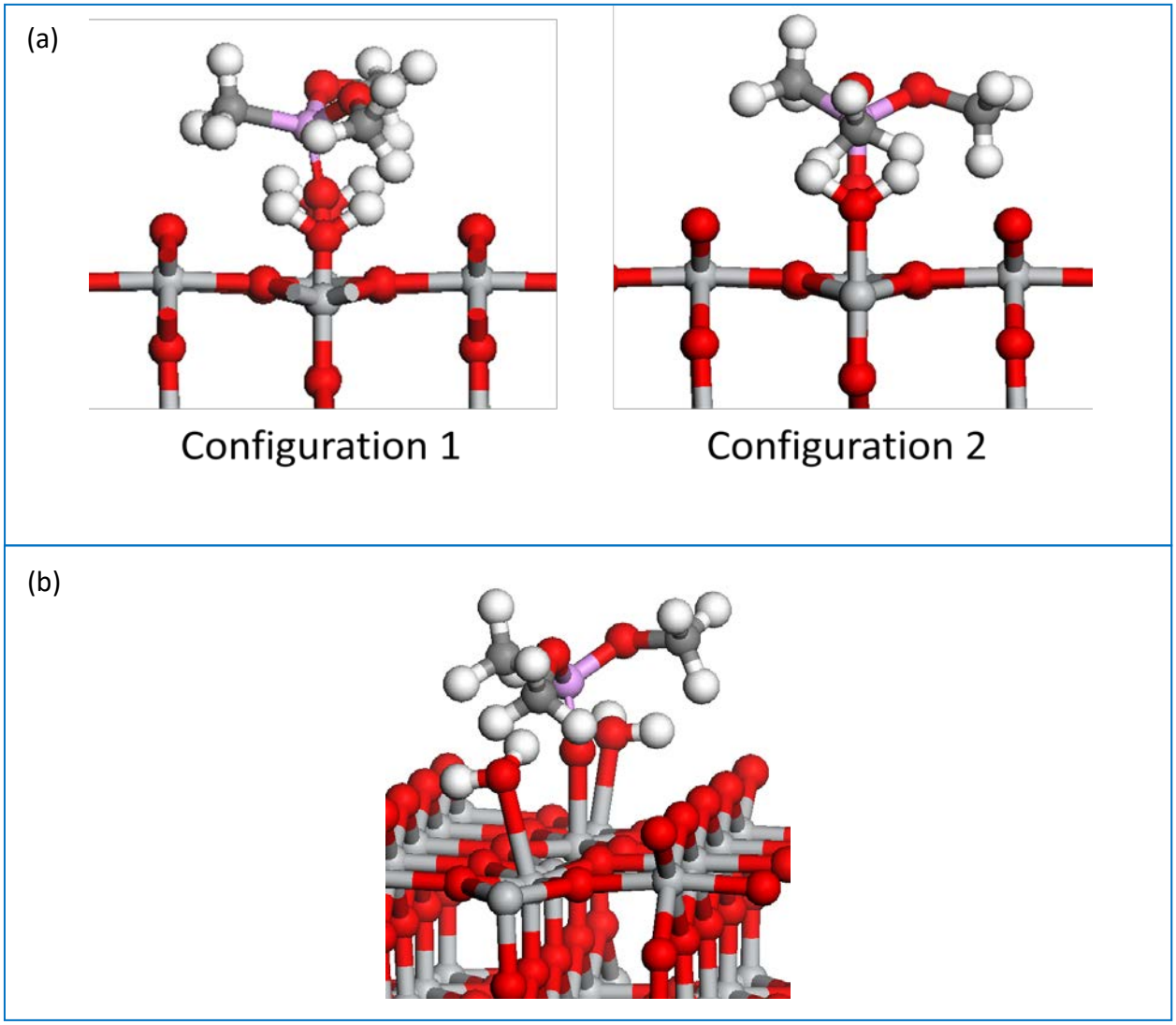

(S7) Molecular adsorption of DMMP on hydrated TiO_2(110) (a) Initial configuration (b) Final most stable configuration

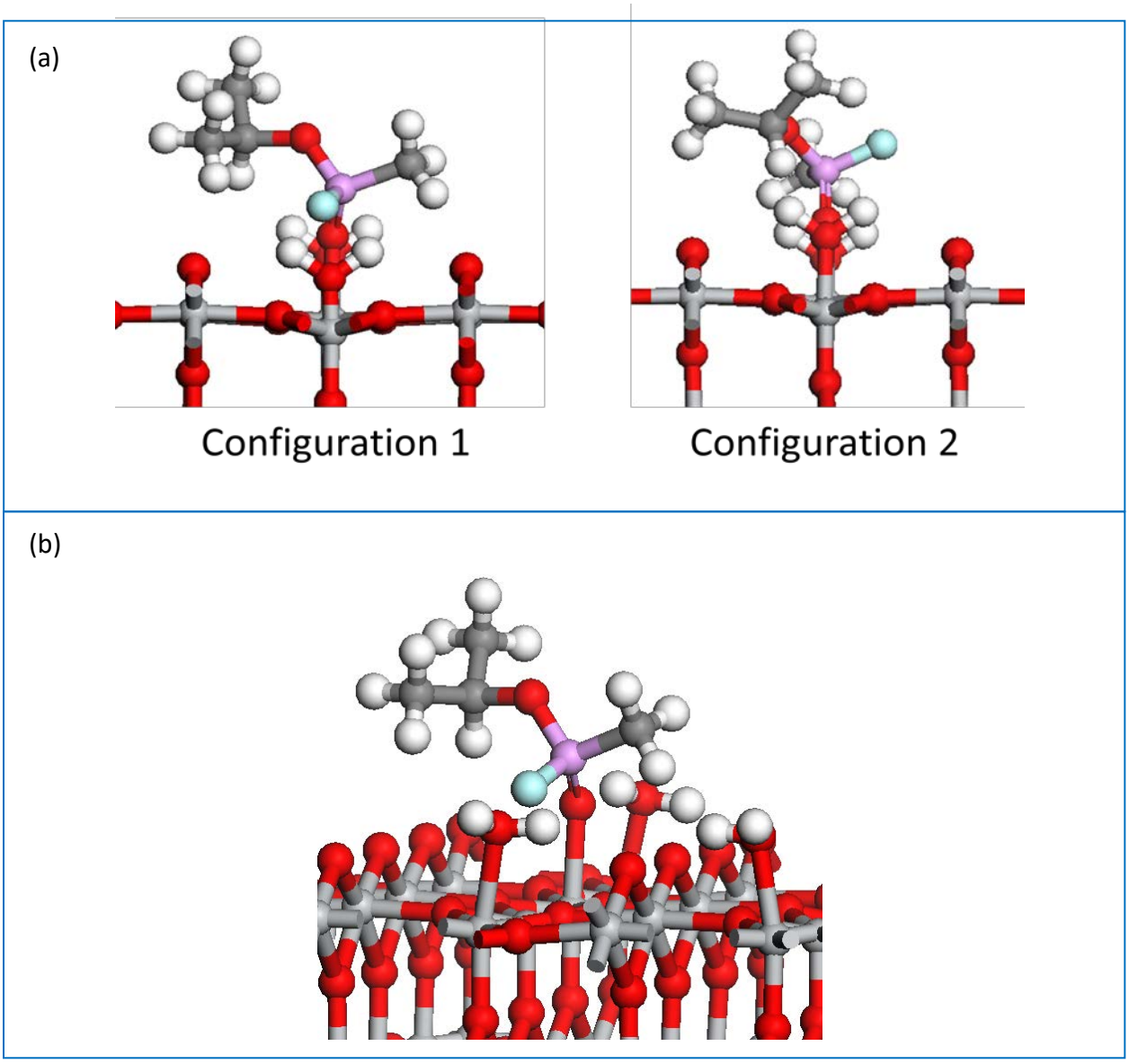

(S8) Molecular adsorption of Sarin on hydrated TiO_2(110) (a) Initial configuration (b) Final most stable configuration

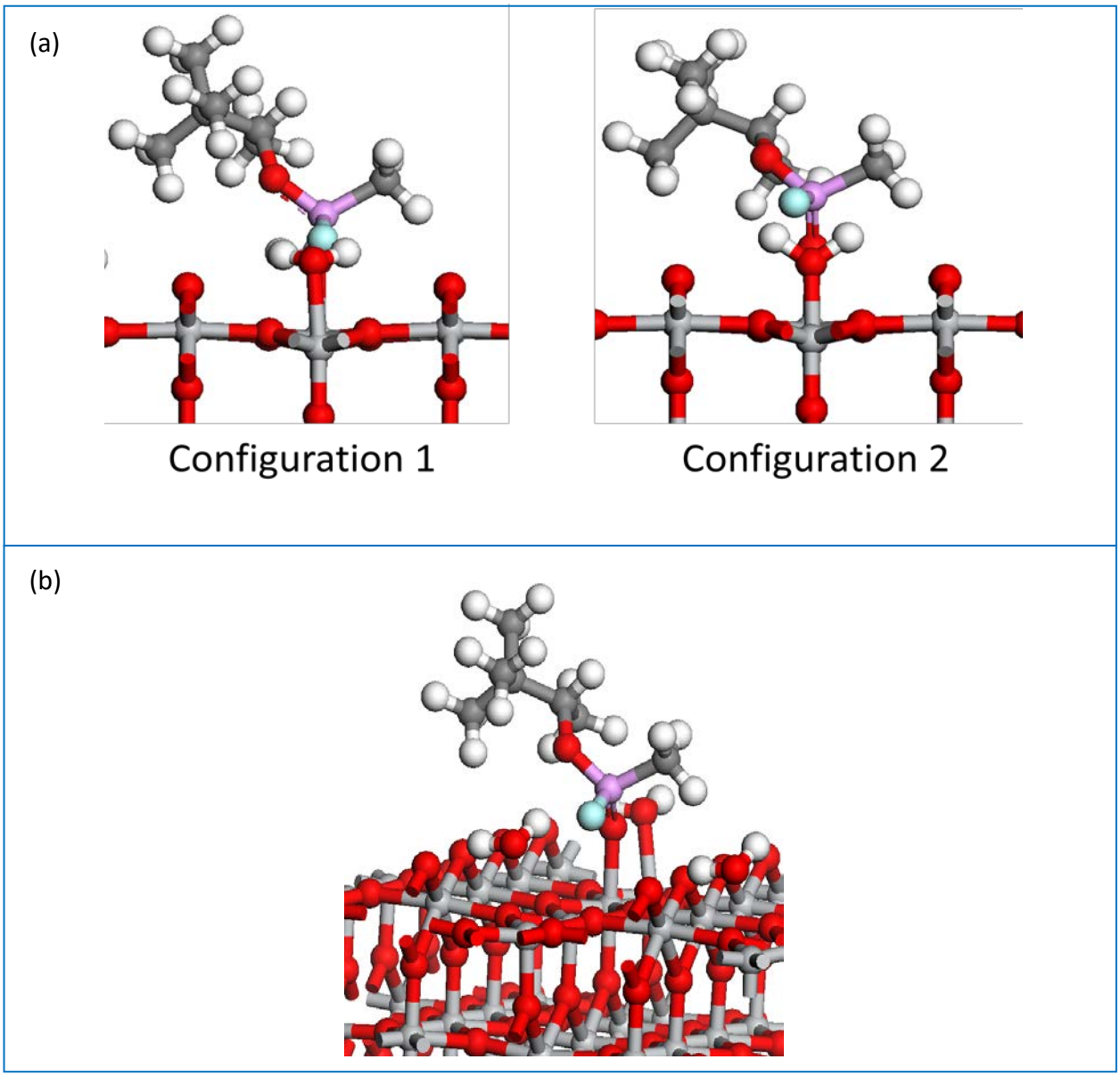

(S9) Molecular adsorption of Soman on hydrated TiO_2(110) (a) Initial configuration (b) Final most stable configuration

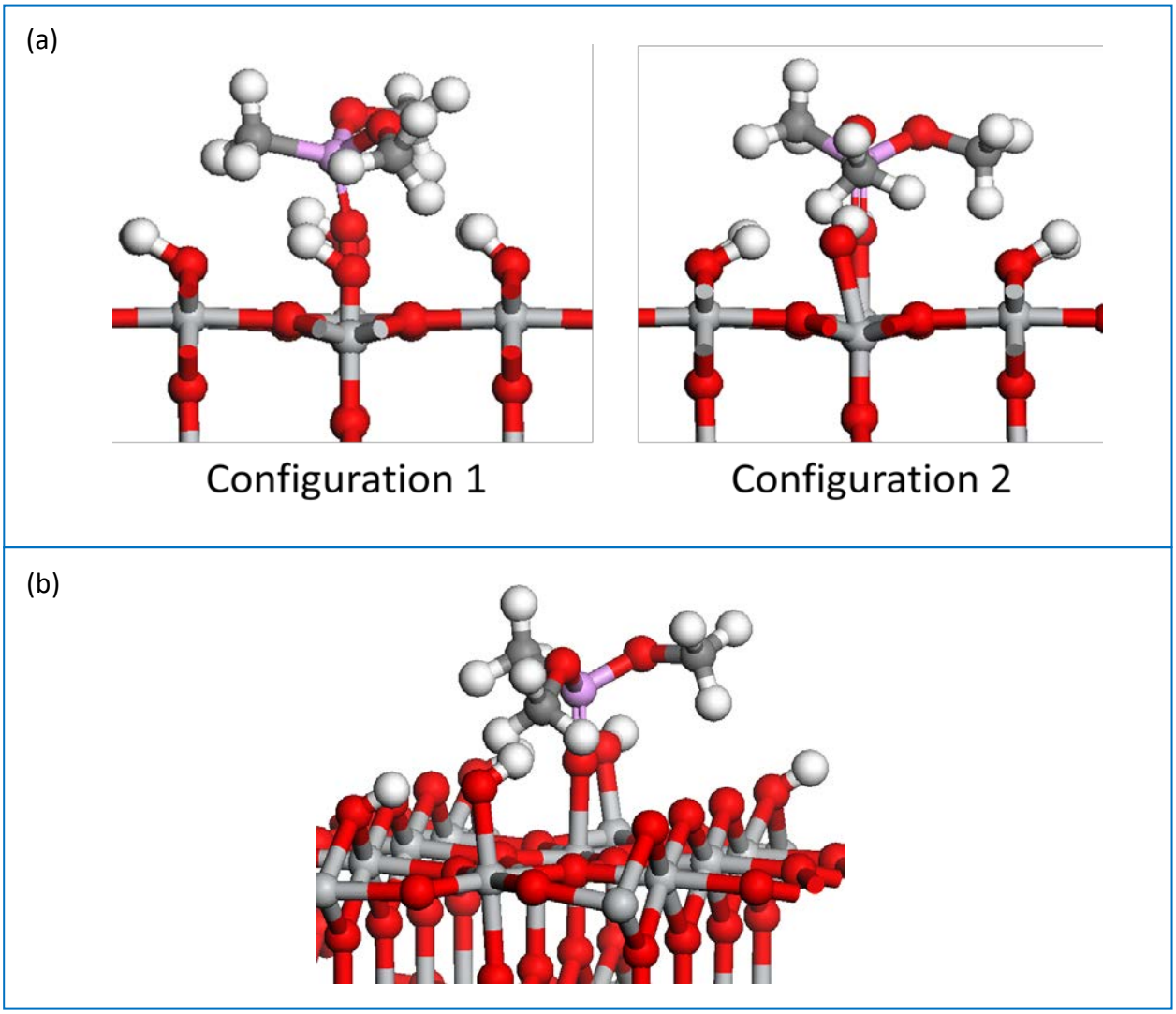

(S10) Molecular adsorption of DMMP on hydroxylated TiO_2(110) (a) Initial configuration (b) Final most stable configuration

(a)

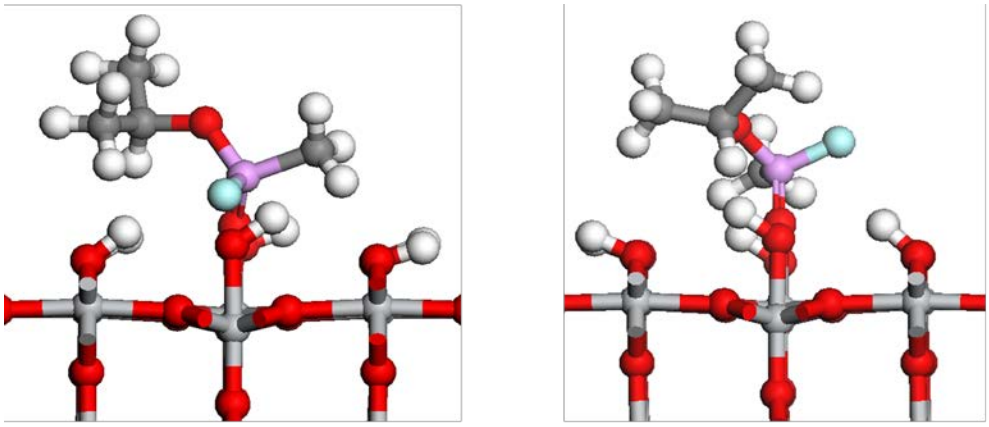

(b)

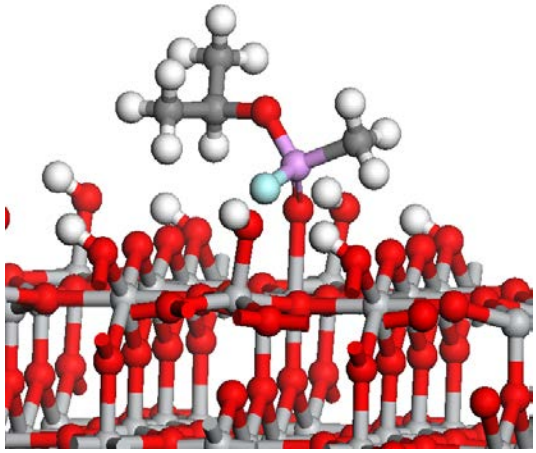

(S11) Molecular adsorption of Sarin on hydroxylated TiO_2(110) (a) Initial configuration (b) Final most stable configuration

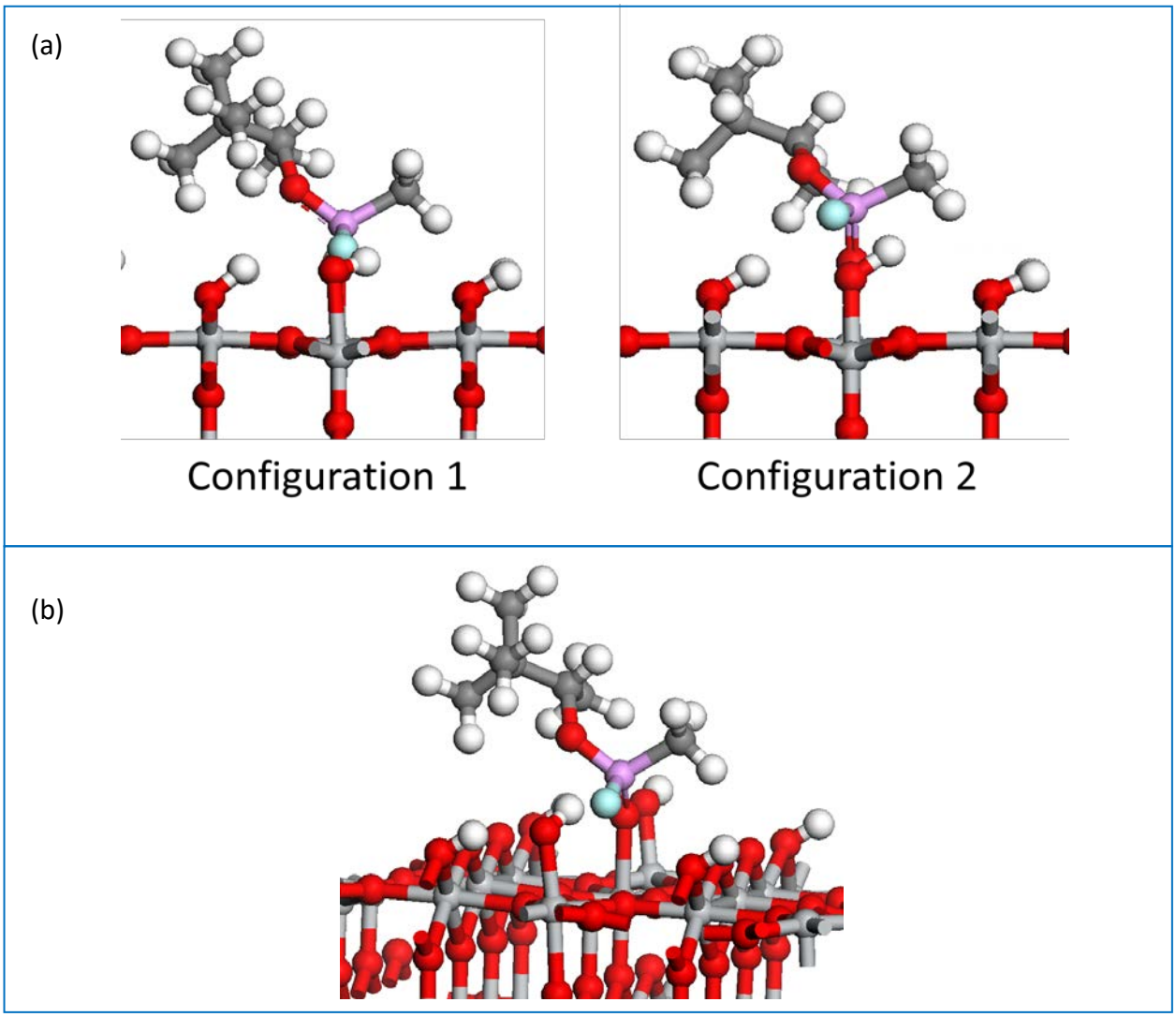

(S12) Molecular adsorption of Soman on hydroxylated TiO_2(110) (a) Initial configuration (b) Final most stable configuration

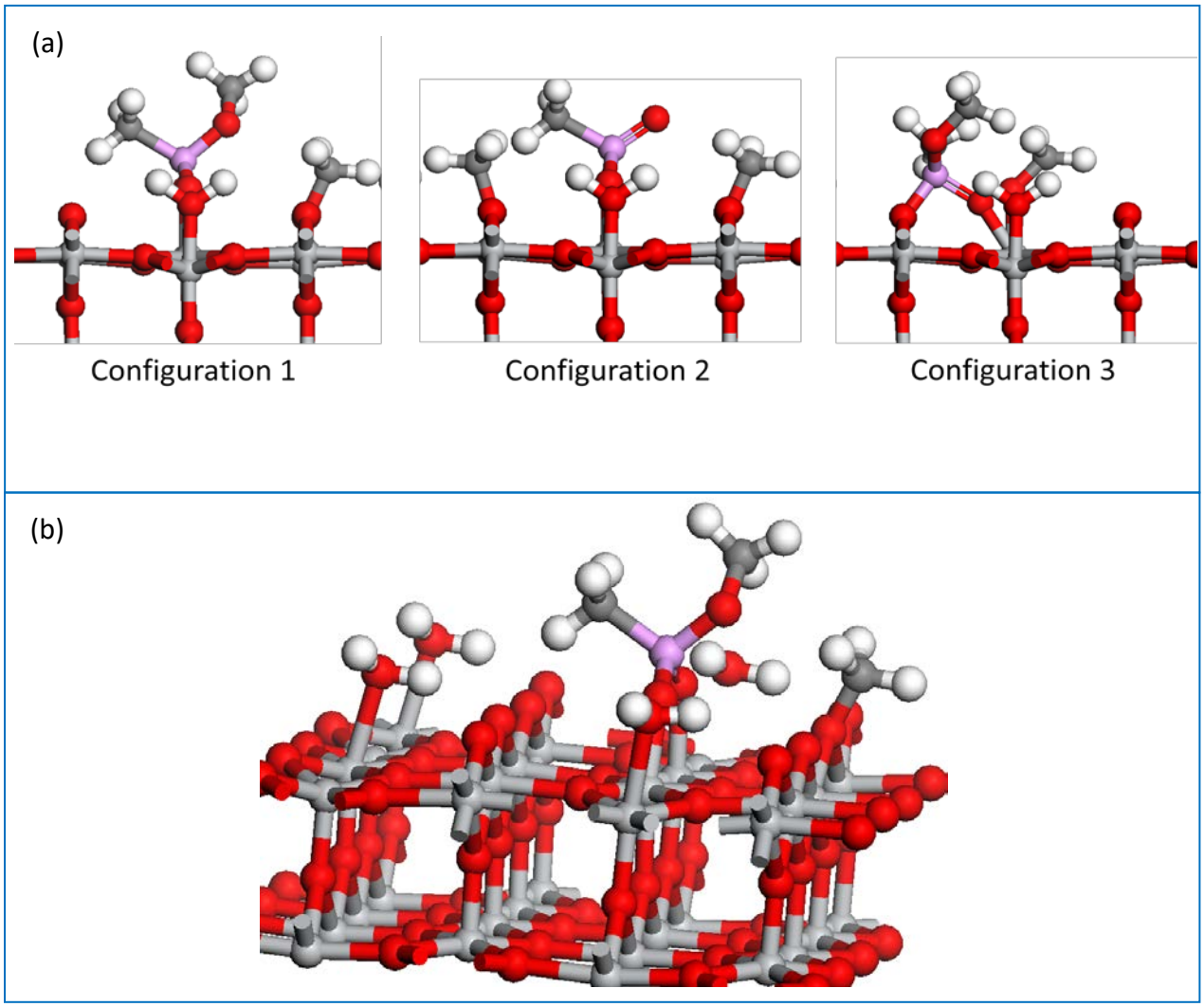

(S13) Dissociative adsorption of DMMP on hydrated TiO_2(110) (a) Initial configurations (b) Final most stable configuration

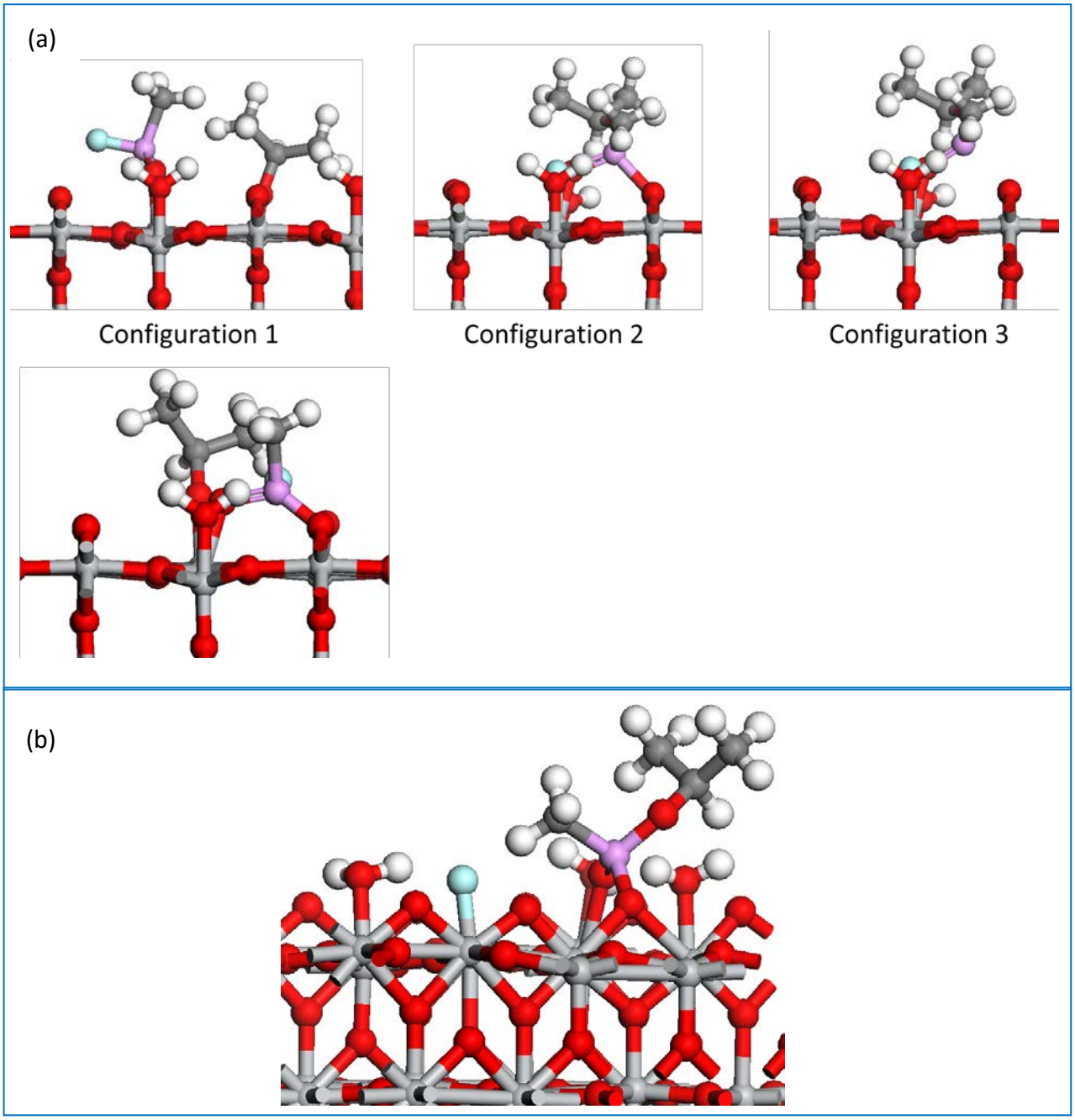

(S14) Dissociative adsorption of Sarin on hydrated TiO_2(110) (a) Initial configurations (b) Final most stable configuration

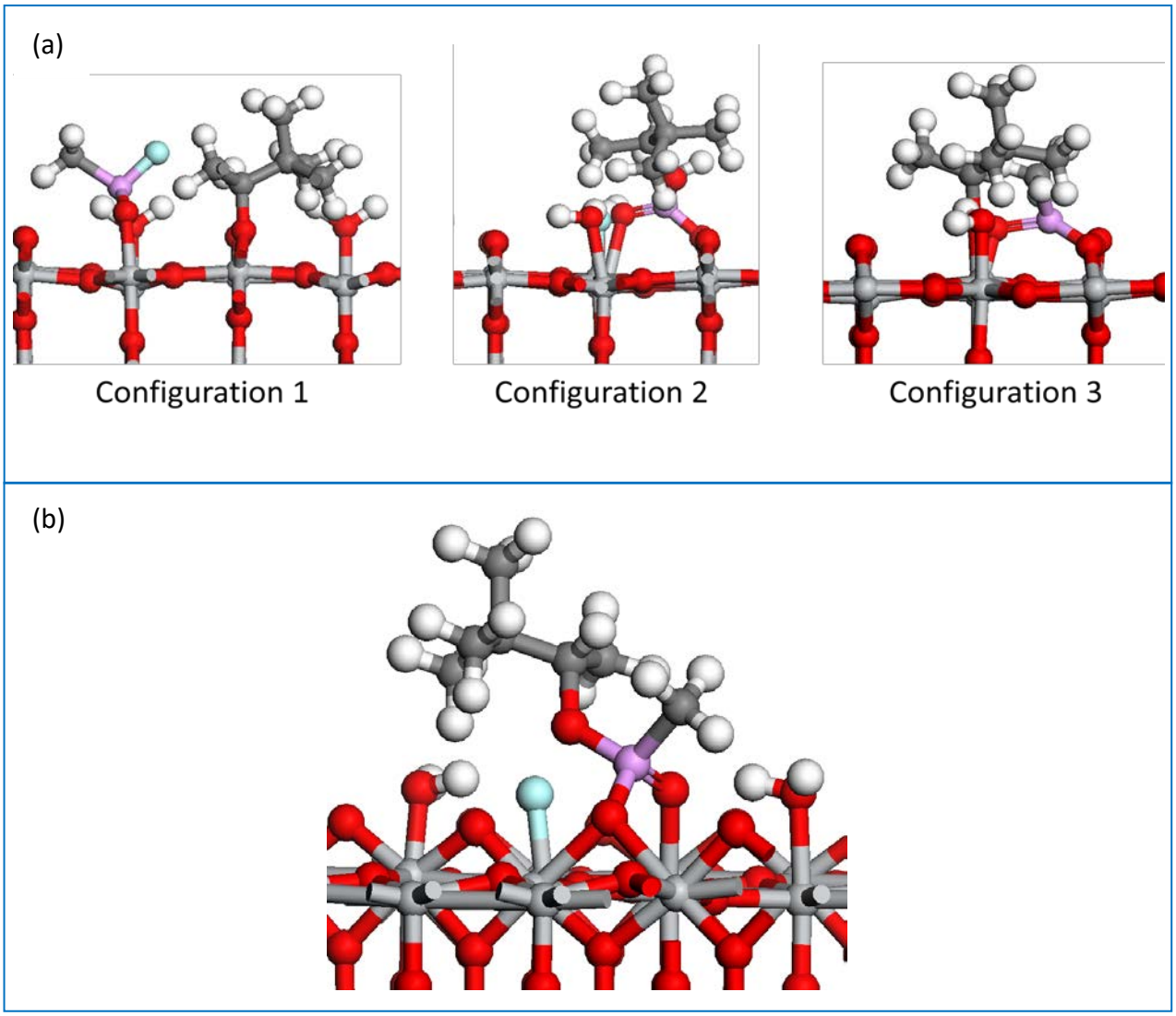

(S15) Dissociative adsorption of Soman on hydrated TiO_2(110) with H_2O in a molecular configuration (a) Initial configurations (b) Final most stable configuration

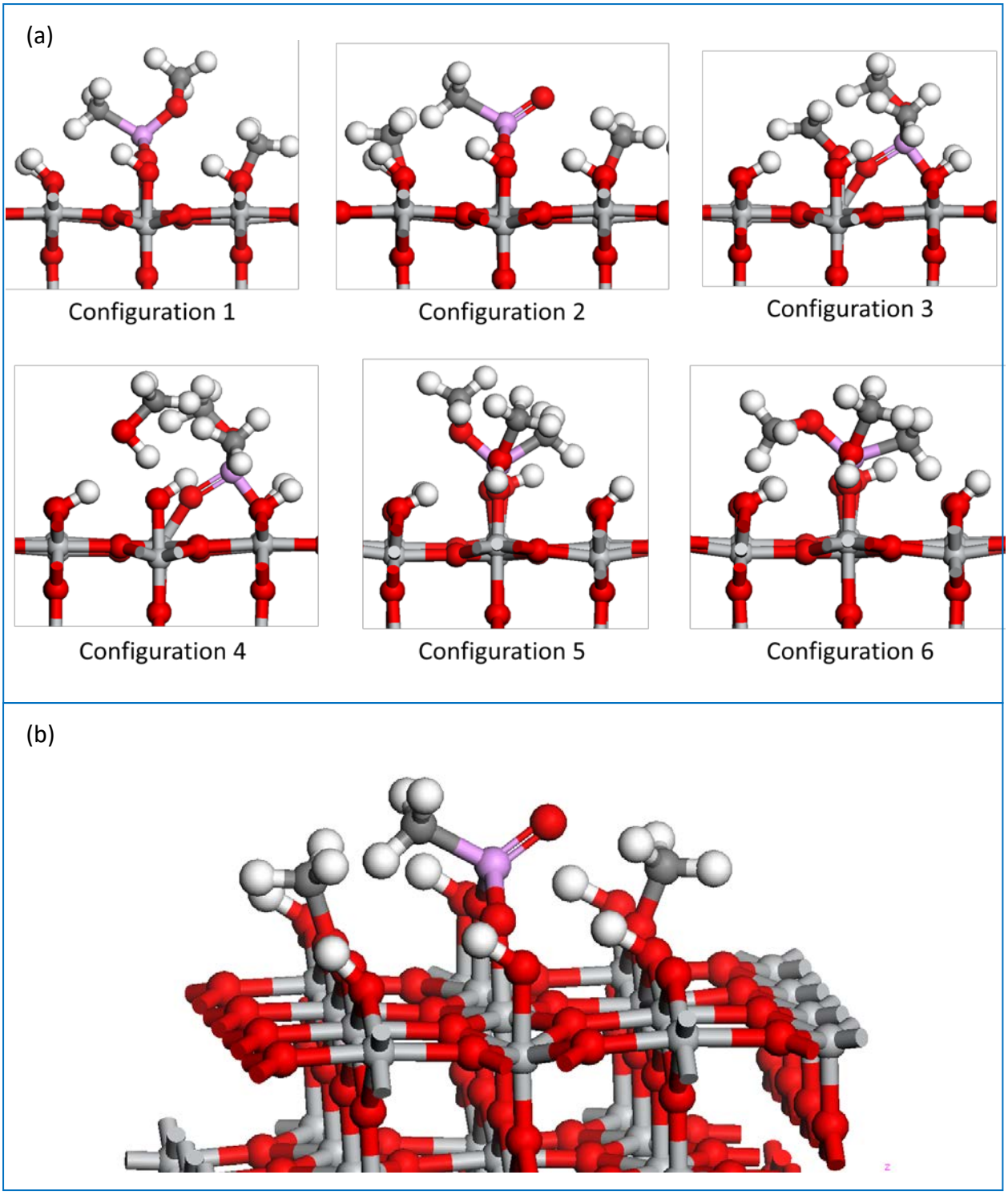

(S16) Dissociative adsorption of DMMP on hydroxylated TiO_2(110) (a) Initial configurations (b) Final most stable configuration

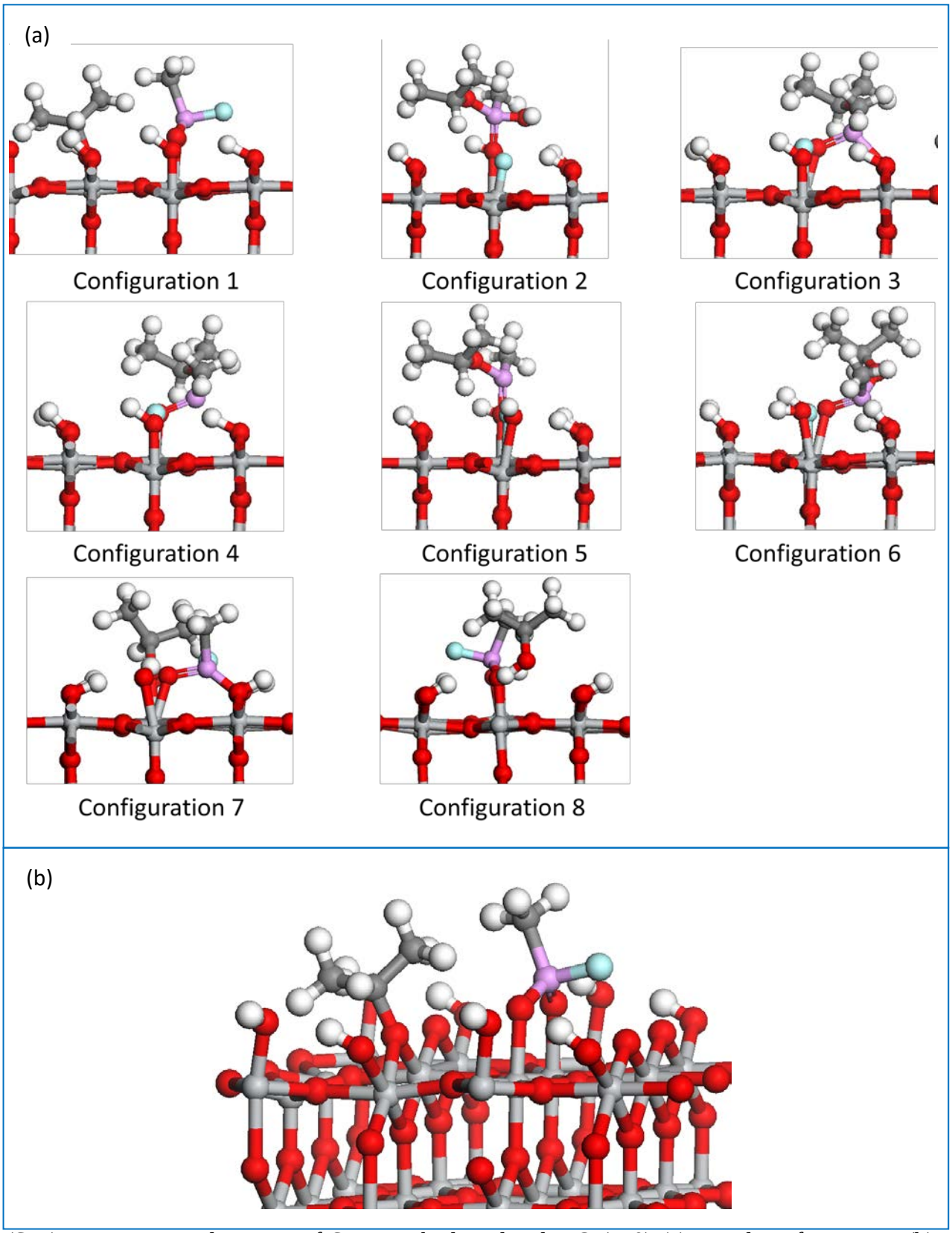

(S17) Dissociative adsorption of Sarin on hydroxylated TiO_2(110) (a) Initial configurations (b) Final most stable configuration

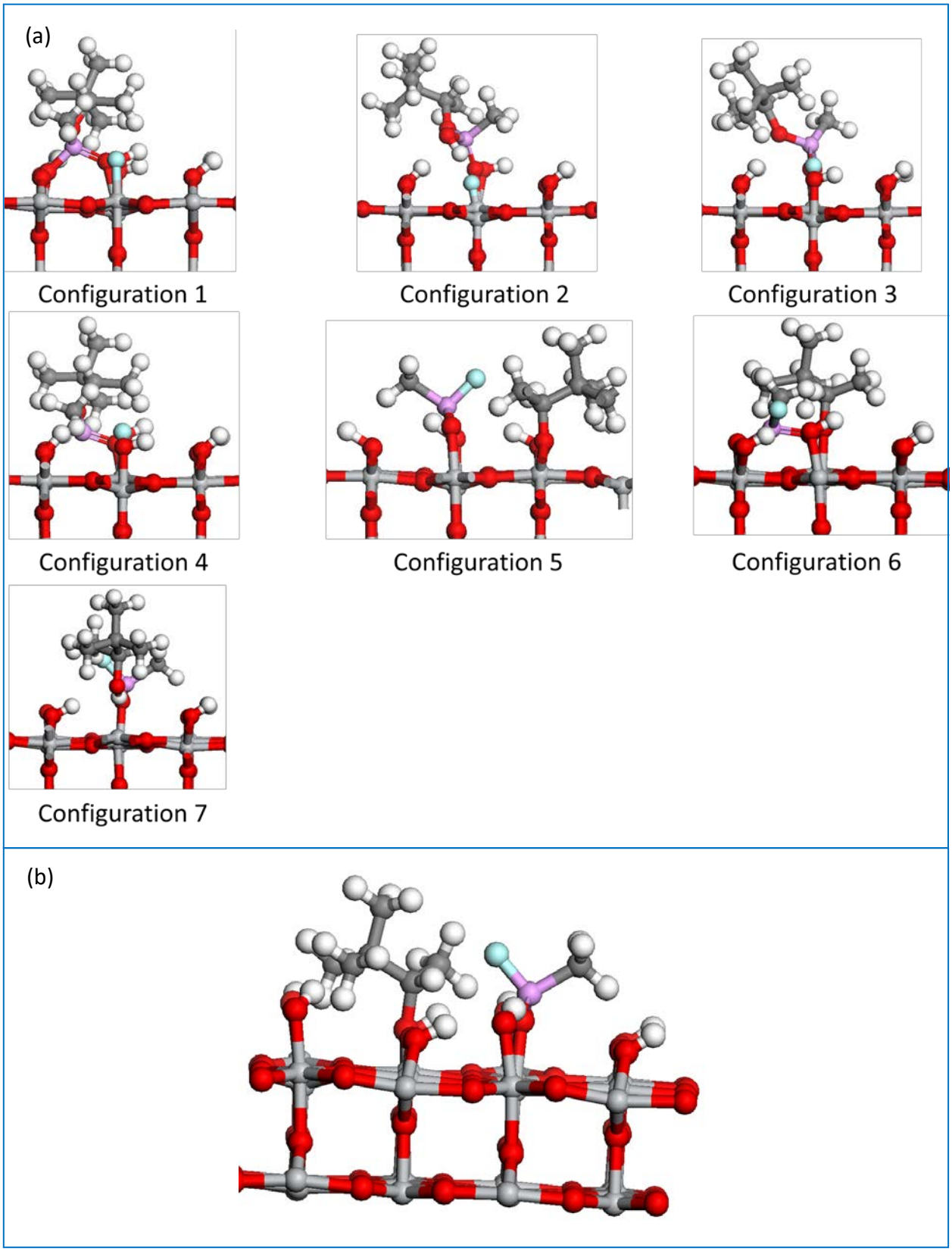

(S18) Dissociative adsorption of Soman on hydroxylated TiO_2(110) (a) Initial configurations (b) Final most stable configuration